Chapter 6 – Plasma Formation and Sustainment

This page intentionally left blank

Chapter 6

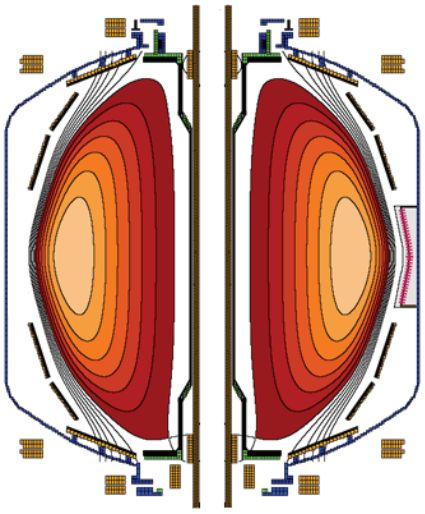

Plasma formation and sustainment

6.1 Overview

The start-up, ramp-up, and sustainment of a tokamak plasma utilizing little or no induction from a central solenoid is a major challenge in magnetic fusion. The development of techniques to minimize or eliminate central solenoid action is critical to the design of compact electricity-producing fusion power plants based on the spherical torus/tokamak (ST) and could also benefit advanced tokamak (AT) reactors. For component testing applications of the ST, the central solenoid flux of ST-CTF is expected to be either zero or inadequate to ramp the plasma to full operating current. Thus, even if some inductive plasma start-up capability is available, non-inductive means of plasma current ramp-up and sustainment are required. Given the scientific and operational challenges of non-solenoidal formation and sustainment, the problem is best solved by dividing it into pieces and addressing issues individually while ensuring that the pieces are ultimately compatible and can be integrated.

This division of the start-up, ramp-up, and sustainment problem is shown schematically in Figure 6.1.1 below. As seen in the figure, four divisions and discharge phases are outlined, and each has received differing degrees of emphasis in NSTX. Coaxial Helicity Injection (CHI) has been the plasma start-up technique tested most extensively on NSTX as described in Section 6.4, and plasma guns, poloidal field

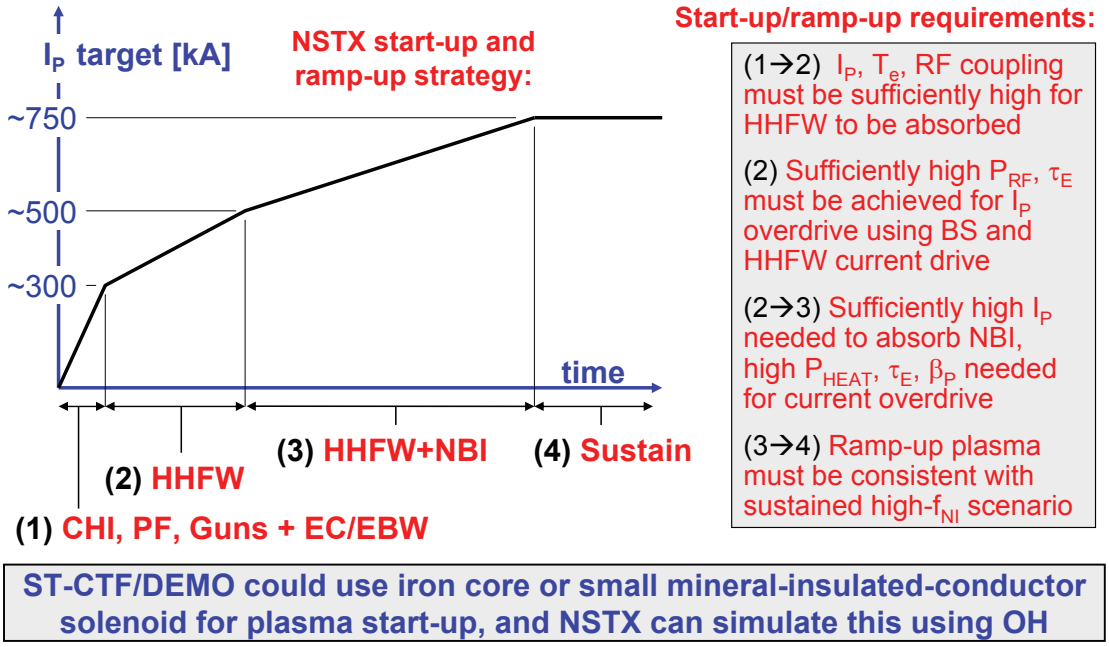

Figure 6.1.1: Division of plasma formation and sustainment problem into 4 distinct pieces as function of time and plasma current: (1) plasma start-up, (2) initial heating and over-drive ramp-up of start-up plasma, (3) additional heating and current drive for additional over-drive to full operating current, and (4) plasma sustainment phase.

start-up, and ECH/EBW start-up are planned to be tested in the five year plan. For plasma current ramp-up from low plasma current, high-harmonic fast-waves have heated 200kA H-mode plasmas to $T_e > 1$keV and generated high bootstrap fractions up to 85%. Increased heating power will be implemented to attempt to increase the bootstrap current > 100% for plasma current ramp-up. For the present NBI sources, NBI power is only well absorbed for plasma currents above approximately 500kA in NSTX, so NBI ramp-up of the plasma current has been tested to only a very limited extent in NSTX. The combination of higher NBI power (from the 2nd neutral beam) and higher toroidal field will enable NBI plasma current ramp-up tests at higher plasma current for which the beam is better absorbed and higher NBI-CD is possible. Finally, for plasma sustainment, up to 70% of the plasma current has been sustained

non-inductively with NBI and BS current drive for plasma currents in the range of 700-800kA. With the major upgrades of NSTX (higher toroidal field and current, 2nd neutral beam for additional power and more tangential injection) combined with density reduction, fully non-inductive and controlled scenarios with plasma currents up to 1MA appear possible. In the sections that follow, progress and plans for plasma formation and sustainment for the 5 year period 2009-13 are provided. Since full non-inductive plasma sustainment is paramount to all next-step ST devices, plasma sustainment is treated first.

6.2 Plasma sustainment results

The NSTX five year goal for plasma sustainment is a demonstration of fully non-inductive current drive (NICD) in a regime consistent with high beta and high confinement that is extrapolable to next-step ST devices such as ST-CTF [1] and NHTX [2]. Next-step ST devices propose to achieve long-pulse/steady-state operation utilizing primarily bootstrap (BS) current and neutral beam injection (NBI) current drive. Other current-drive sources such as Electron Bernstein Wave (EBW) CD also appear promising for off-axis CD and profile control [3] in the over-dense plasmas of the ST and are under active investigation [4].

Fully non-inductive operation has not yet been demonstrated on any ST device, and full-NICD operation at or above the no-wall limit and with high confinement is extremely challenging for all tokamaks. DIII-D has transiently achieved fully non-inductive operation at high performance utilizing NBI + BS + ECCD, but with un-relaxed profiles [5]. As another example, a reasonably high level of non-inductive current drive (NICD) of approximately 70% has only recently been achieved on JET using NBI and BS [6], and only through operation above the no-wall stability limit [7] utilizing rotational stabilization of the RWM much like NSTX [8] and DIII-D [9]. As shown in Figure 6.2.1, NSTX has made significant progress operating far above the n=1 no-wall limit and near the n=1 ideal-wall limit and with H-mode confinement enhancement factor H_{98pby2}=1.0-1.1 sustained for up to several current redistribution times [10,11]. In these plasmas, approximately 55% of current is provided by the bootstrap current, and 10-15% is provided by NBI-CD, resulting in 65-70% non-inductive current fraction. Also as shown in Figure 6.2.1, the predicted and reconstructed current profiles are in good agreement during periods when the discharges are MHD-quiescent, but there is also evidence that NBI fast-ions and the NBI current drive can be redistributed when large core MHD activity is present [12].

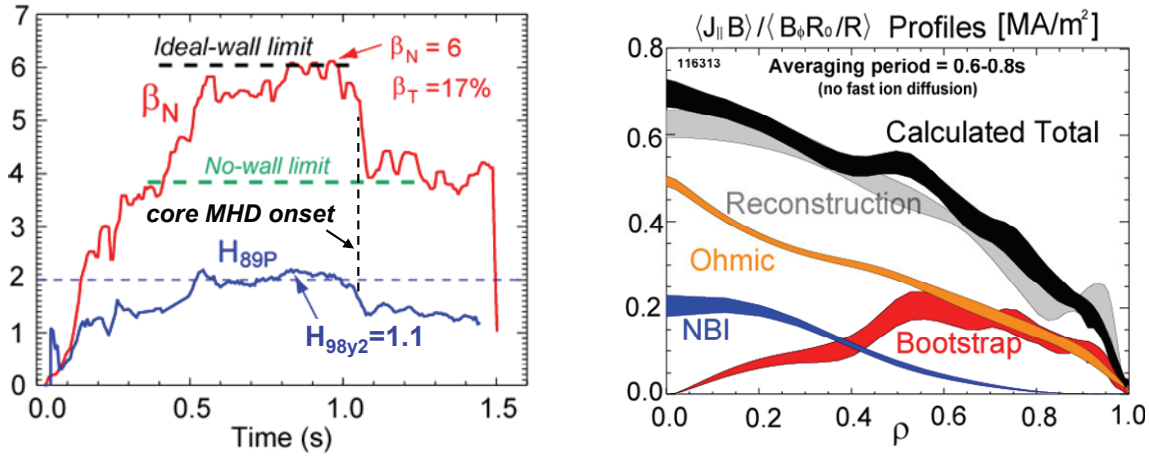

Figure 6.2.1: (Left) Example of integrated high performance discharge 116313 with β_N near the ideal wall limit, β_T =15-20%, and high confinement at or above the ITER-98y2 H-mode scaling projection. The high performance phase is sustained for 1.5-2 current redistribution times and 10-15 energy confinement times. The high performance phase is interrupted by core n=1 kink/interchange activity triggered by the q profile evolving toward q_{min} = 1 and repeated transient excursions above the ideal-wall limit. (Right) Demonstration of good agreement between predicted current profile (including inductive and non-inductive sources) and the reconstructed current profile constrained by the MSE data.

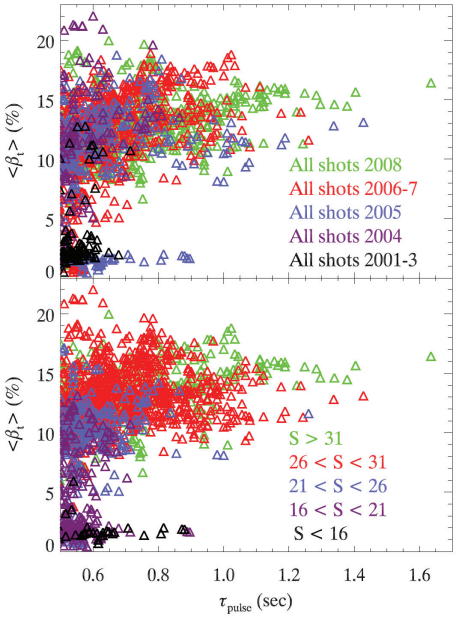

Figure 6.2.2: (Top) shot flat-top-average toroidal beta vs. flat-top duration sorted by year, (bottom) sorted by shaping factor $S \equiv q_{95}\, aB_T / I_P$ [m•T/MA].

As described in Chapter 2 on NSTX Macroscopic Stability, the plasma shaping capability of NSTX has been systematically improved during the last five year period through the replacement of 2 divertor coils to increase the plasma triangularity at high elongation. The elongation has also been increased by taking advantage of reduced latency in the plasma control system, as described in Chapter 7.

As shown in Figure 6.2.2, plasma shaping factor is clearly important in increasing the duration of sustained high plasma beta. Strong plasma shaping can also play an important role in the early discharge evolution by modifying the current profile during the

plasma current ramp. In particular, increased elongation early in the discharge enables the plasma to be diverted earlier. Increased elongation and triangularity at fixed current increase the magnetic safety factor, and early diverting can improve plasma confinement by enabling early H-mode access. As shown in Figure 6.2.3, increased early shaping (κ = 1.9 → 2.2 and δ_L = 0.4 → 0.8) and early diverting can significantly increase the minimum q in the plasma and reduce the internal inductance by as much as 25%. By delaying the approach of q_{min} toward 1 with strong early shaping, deleterious MHD activity is reduced or avoided increasing discharge pulse-length and the duration of sustained high beta.

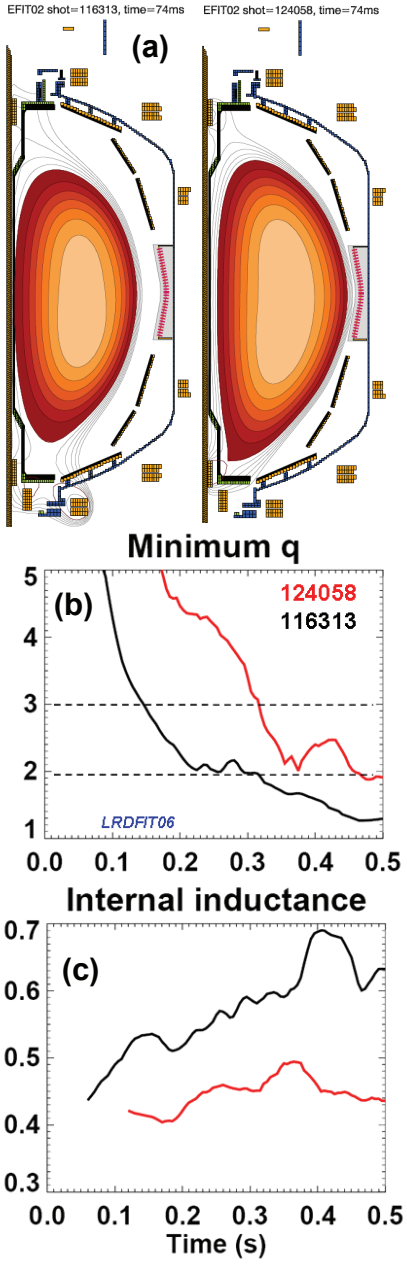

Figure 6.2.3: (a) Comparison of boundary shapes at t=74ms during the plasma current ramp without (left) and with (right) increased early elongation, and comparison of (b) minimum q and (c) internal inductance evolution.

In 2006-2008, error field correction was also optimized and utilized routinely in an increasing number of discharge scenarios. In particular, it was found that both n=1 and n=3 error fields are present in NSTX. In the recently implemented EF correction system, the amplification of n=1 error fields (resonant field amplification – RFA) is measured and compensated in real-time. The n=1 RFA suppression algorithm is also effective at actively stabilizing resistive wall modes (RWM) when the plasma rotation is insufficient to stabilize the n=1 RWM. The optimal n=3 error field correction is presently pre-programmed and is apparently indicates the n=3 intrinsic error field is proportional to the PF5 vertical field current. In 2007, n=3 error field correction was shown to aid in the sustainment of high plasma rotation and high beta, and when combined with active n=1 control, can aid

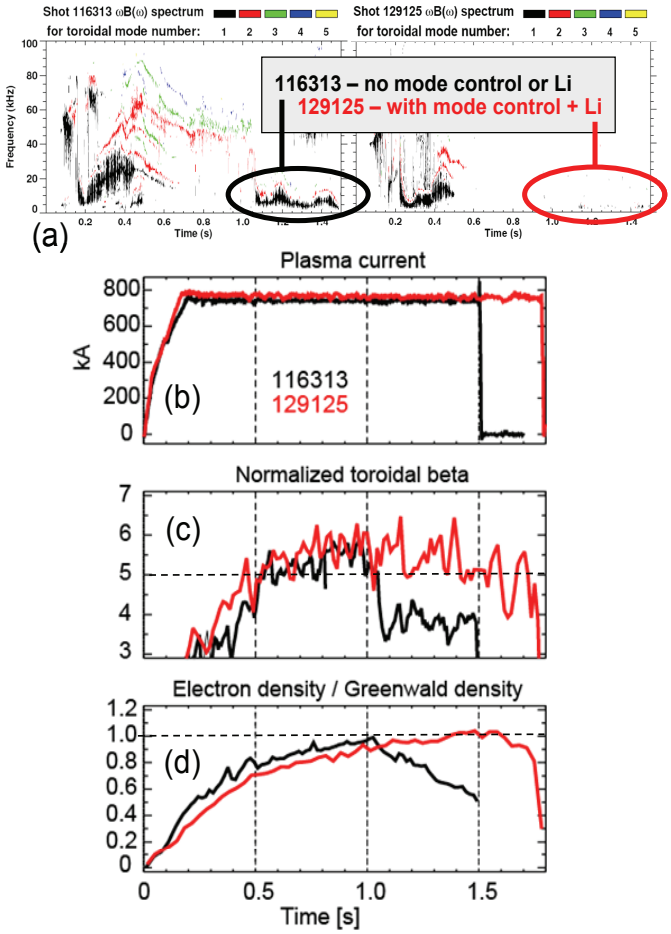

Figure 6.2.4: (a) Elimination of late n=1 MHD mode activity by combination of n=1+n=3 EF correction and lithiumization, (b) achievement of NSTX record pulse-length = 1.8s, (c) sustainment of β_N > 5 for 1.1s = 3-4 current redistribution times – doubling the duration of the previous record, and (d) Greenwald density fraction evolution.

the sustainment of very high performance discharges in NSTX.

As shown in Figure 6.2.4, plasmas utilizing this multiple mode-number (n=1 and n=3) MHD control (in combination with the after-effects of evaporated lithium on the plasma facing components (PFCs)) have achieved record pulse-lengths in NSTX, and the duration of sustained high normalized beta has been doubled relative to that of Figure 6.2.1. For the record pulse-length discharge, Figure 6.2.5 shows that after t=0.8s the MSE pitch angle profile changes very little as a function of time. This result indicates that the current profile has reached a near-equilibrium state. The inductively-driven current fraction is estimated to be 35-45% in this discharge. Equilibrium reconstructions show that the minimum q value in the plasma is constant in time and in the range of 1.2-1.3 after t=0.8s – consistent with the absence of deleterious n=1 MHD activity commonly observed when the minimum q is near or below 1. Overall, improvements to the plasma start-up including early H-mode access [13,14] and early shaping combined with strong shaping in the flat-top, improved error field correction [15], and improved wall conditioning [16] have increased the pulse duration at high performance by a factor of 2 to 3 relative to the beginning of the previous 5 year plan which began in 2004.

From these results, it appears that most core plasma parameters of interest can achieve nearly steady-state conditions in NSTX discharges. However, Figure 6.2.4d shows that the plasma density does not reach steady-state conditions in this discharge, but rather continues to increase monotonically toward a Greenwald density ratio of approximately 1 by t=1.5s. Near this time, the high-β phase of the discharge is interrupted by the onset of large ELMs and a reduction in confinement. Similar density rises are observed in nearly all high performance H-mode discharges in NSTX.

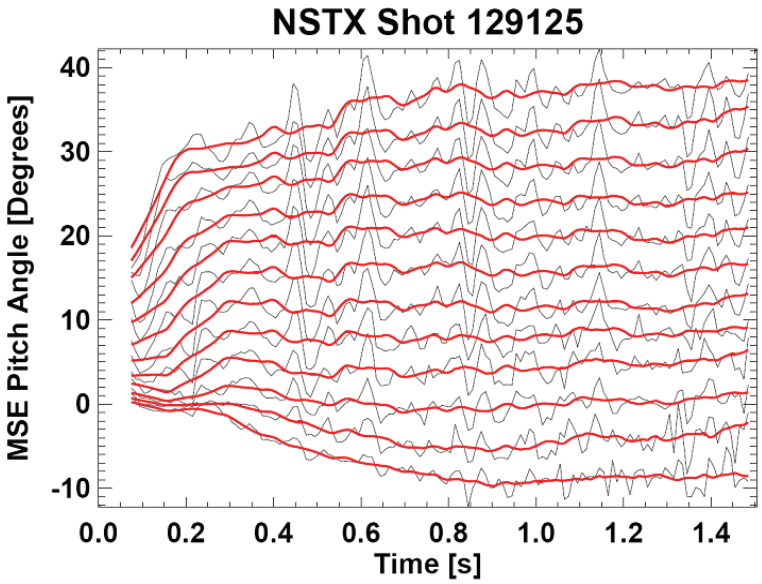

Figure 6.2.5: MSE pitch angle evolution of NSTX long-pulse discharge 129125 showing equilibration of the plasma current density profile after t=0.8s. Black is measured pitch angle (modulated by ELMs) and red is the time-smoothed pitch angle.

Improved density control would enable the achievement of more stationary plasma conditions, would enable controlled experiments as a function of density, and would increase the fraction of beam-driven current drive as proposed for next-step ST devices operating with 100% non-inductive current drive. As a result, achieving density control is major emphasis of the NSTX 2009-13 5 year plan. Furthermore, to achieve fully non-inductive current drive in NSTX, the inductive current-drive described above must be replaced by other non-inductive sources. During the next five year period, is not anticipated that sufficient EBW coupling efficiency and/or heating power will be available to provide bulk non-inductive current drive in NSTX. Because of this, and because of the heavy reliance of NBI-CD and BS-CD in the proposed operating scenarios of next-step ST devices, NSTX will focus on increasing the bootstrap and beam-driven currents by all available means.

6.3 Plasma sustainment plans

6.3.1 Overview

As described above, testing and demonstrating the viability of operating an ST-based magnetic confinement device without inductive current drive is a major goal for the next 5 years. Increased neutral beam and bootstrap current drive are the primary tools proposed for achieving this goal. A critical

GOALS: reduce n_e, increase NBI-CD, increase thermal confinement

Present high β_N & f_{NICD}	NSTX	NHTX	ST-CTF
A	1.53	1.8	1.5
κ	2.6-2.7	2.8	3.1
β_T [%]	14	12-16	18-28
β_N [%-mT/MA]	5.7	4.5-5	4-6
f_{NICD}	0.65	1.0	1.0
$f_{BS+PS+Diam}$	0.54	0.65-0.75	0.45-0.5
f_{NBI-CD}	0.11	0.25-0.35	0.5-0.55
$f_{Greenwald}$	0.8-1.0	0.4-0.5	0.25-0.3
H_{98y2}	1.1	1.3	1.5
Dimensional/Device Parameters:			
Solenoid Capability	Ramp+flat-top	Ramp to full I_P	No/partial
I_P [MA]	0.72	3-3.5	8-10
B_T [T]	0.52	2.0	2.5
R_0 [m]	0.86	1.0	1.2
a [m]	0.56	0.55	0.8
I_P / aB_{T0} [MA/mT]	2.5	2.7-3.2	4-5

Table 6.3.1: Comparison of key dimensionless and dimensional parameters of present high non-inductive current fraction scenarios in NSTX, and those proposed for NHTX and ST-CTF.

element in making progress toward this goal is to identify and reduce the key operational and scientific gaps between present ST performance and the performance assumed in next-step ST device designs.

Table 6.3.1 shows a comparison of key dimensionless and dimensional parameters of present high non-inductive current fraction scenarios achieved in NSTX, and those proposed for NHTX and ST-CTF. This table shows that several parameters in next-step ST designs have been nearly achieved or even exceeded in NSTX plasmas – in particular the elongation, normalized beta, and bootstrap fraction. However, from this table, it is evident that the beam driven current fraction is lower than assumed in next-step ST designs

by a factor of 2 to 5, the normalized plasma density is higher than assumed by a factor of 2 to 3, and the H-mode confinement enhancement factor must be increased by up to 35%. Since NBI-CD efficiency is proportional to T_e / n_e, if the electron pressure remains constant as the electron density is varied, the NBI-CD efficiency would be proportional to $1 / n_e^2$. Thus, reduced electron density is projected to be a very important means of increasing the beam-driven current. However, if anomalous electron transport is determined by micro-instabilities with a critical gradient threshold for instability, the electron temperature profile may be stiff and may not increase as $1 / n_e$ as the density is reduced. Thus, additional means of increasing beam current drive efficiency are warranted.

As discussed in Chapter 3, unlike the scaling observed in standard aspect ratio tokamaks, the electron energy confinement in STs scales nearly linearly with toroidal magnetic field. While the origin of this scaling remains unclear, this scaling does highlight the potential importance of increased toroidal field in increasing beam current drive by increasing the electron temperature. Another important means of increasing the beam-driven current is more tangential injection of the beams as has been proposed in the designs of next-step ST devices. As discussed below, for NSTX, more tangential injection (R_{TAN} up to 1.3m versus present R_{TAN} = 0.5 to 0.7m) is computed to increase the beam current drive efficiency by up to a factor of 1.5 to 2 while also providing off-axis current drive to aid in sustaining $q_{min} > 1$ to avoid deleterious core MHD activity. Thus, density reduction via pumping, higher toroidal field and current, and more tangential beam injection are the proposed means to increase the NBI current drive in NSTX.

Another key goal is increased thermal energy confinement. This is a very challenging goal, as transport is less directly controllable and improvable in general. Since electron transport is the dominant loss channel in NSTX high-performance H-modes, improvements in electron confinement are essential. Reduced electron thermal diffusivity has been observed in ST plasmas through modifications to the plasma safety factor profile – in particular shear reversal in the plasma core [17]. Utilizing the more tangentially injecting 2nd NBI proposed for NSTX, the degree of shear reversal can be controlled over a range of Δq = 0.5 to 1, and this could in principle increase the core electron temperature and confinement while also increasing the beam current-drive efficiency. Lithium conditioning of the plasma facing components (PFCs) has also been demonstrated to increase thermal confinement in NSTX H-modes [11], and reduced recycling from liquid lithium PFCs has led to dramatic improvements in energy confinement in the CDX-U tokamak [18].

6.3.2 Near-term plans for improved plasma sustainment – FY2009-2011

Increased toroidal field capability from a new centerstack, and improved NBI current-drive efficiency and profiles from a 2nd NBI are longer-term major upgrade objectives of the NSTX research program. In the nearer term, NSTX research will focus on density reduction and understanding and utilizing the potential benefits of liquid lithium. Liquid lithium has been shown to be a very efficient pump of D, and this motivates an integrated approach to achieving the density control and confinement improvement goals of NSTX. In particular, NSTX will implement a Liquid Lithium Divertor (LLD) in 2009 as shown in Figure 6.3.1. This is a unique capability in the world program, as NSTX will be the only diverted H-mode tokamak using liquid lithium PFCs. More details of the design of the LLD are given in Chapter 7. The surface area of the LLD has been chosen to provide the needed pumping to reduce the electron density by 25% (for high triangularity δ_{Lower} = 0.6-0.8 shapes) to up to 50% (for lower triangularity shapes). This projected degree of density reduction is consistent with increasing the NBI-CD efficiency by a factor of 2 to 4, depending on whether the electron temperature is constant or increases with decreasing density.

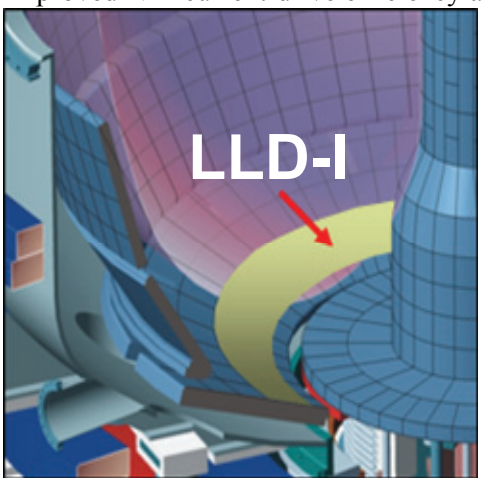

Figure 6.3.1: The NSTX liquid lithium divertor target plate – version 1 (LLD-I) will be located on the outboard divertor of NSTX and is planned to be operational during the FY2009 campaign.

Integrated modeling with the TSC code has been performed [19] to identify approaches to increasing the non-inductive current fraction with the tools presently available on NSTX. The parameters of the two approaches that appear most promising at the present time are summarized in Figure 6.3.2 below. Approach #1 (as described above) reduces the density to increase NBI-CD and thereby increases the non-inductive current fraction to up to 90%. However, because of the centrally peaked NBI-CD profile driven by the present NBI system, the resulting total current density profile is projected to be non-stationary and to reach an unstable equilibrium with $q_{min} < 1$ unless the fast-ions are redistributed by MHD activity. Approach #2 utilizes an elevated core safety factor (q(0) = 1.4 to 2.4) to increase the beta limit, and relies on higher confinement from LLD and/or heating power from HHFW to produce a high bootstrap fraction

plasma at electron density values below but comparable to those presently achieved. Thus, at the very least, both approaches require electron density reduction. Approach #1 with low density and high NBI-CD fraction is most similar to the proposed operating scenario of an ST-CTF, whereas approach #2 with increased bootstrap fraction is closer to the proposed operating scenario of NHTX.

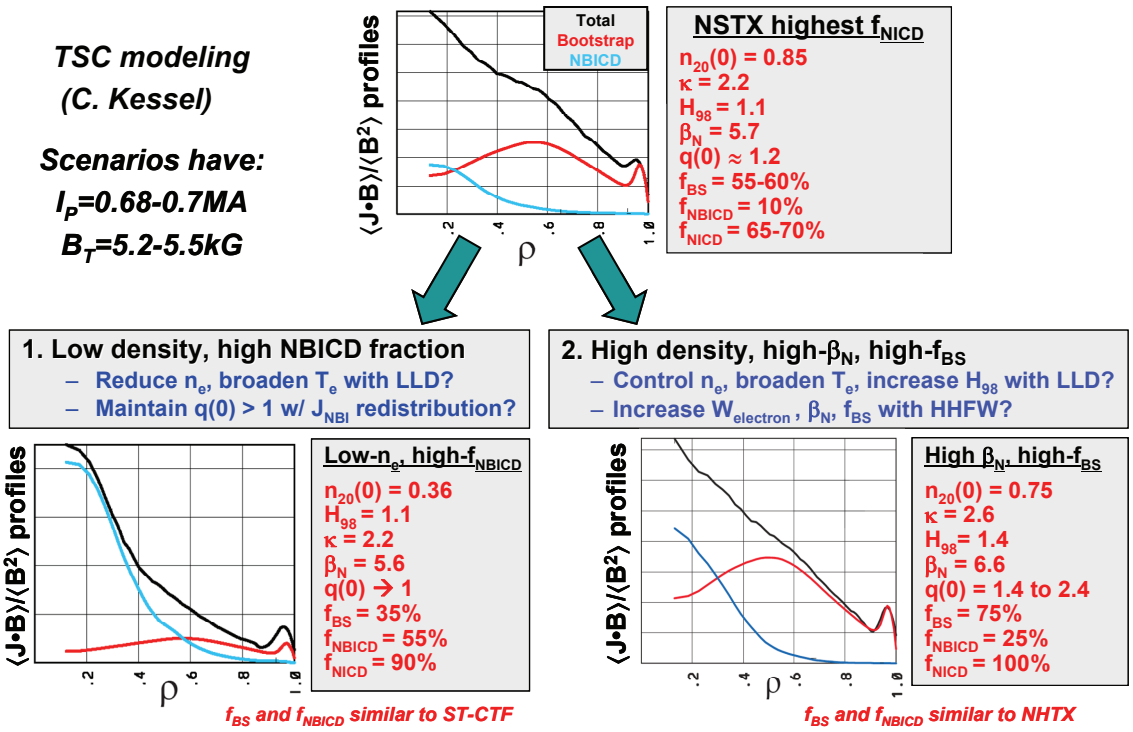

Figure 6.3.2: Comparison of key parameters and current profiles of present NSTX performance (top) and two operational scenarios proposed to increase the fraction of non-inductive current drive (bottom).

Unlike the ST-CTF and NHTX scenarios which are projected to operate near the no-wall stability limit, both NSTX approaches described here require operation above the no-wall stability limit and would rely on the MHD control techniques already developed successfully on NSTX. This difference in stability (i.e. normalized beta) results from NSTX scenarios targeting operation at toroidal beta values comparable to those of next-step STs but at lower normalized current I_P/aB_T. The lower normalized current operation of NSTX is due in part to the lower normalized NBI-CD efficiency resulting from the more perpendicular beam injection of NSTX, and is also due in part to operation at somewhat lower elongation in NSTX than is assumed in next-step STs. The plan for testing these two approaches is given below.

1) Plan for developing low density, high NBI-CD fraction scenario

FY2008 results: Characterized non-inductive current-drive fraction versus density, shaping, q

i) Increased D pumping via more Li + more complete coverage using dual-LITER

ii) Increased beta-poloidal from 1.5 to 1.8 by operating at higher β_N at high elongation

iii) Improved fueling control using super-sonic gas injector (SGI) during I_P ramp phase

b) FY2009-11 Plans

i) Characterize D pumping with dual-LITER plus LLD-I and LLD-II

(1) Perform FY09 milestone on gas balance and particle retention

ii) Study pedestal and ELM stability vs. pedestal collisionality and Lithium (FY10 milestone)

(1) Further test and understand ELM suppression observed with lithium from LITER

iii) Characterize NBI J(r) redistribution from fast-ion and low-frequency MHD (FY09 milestone)

2) Plan for developing high normalized beta, high bootstrap fraction scenario

FY2008 results:

i) Assessed confinement, ELM, thermal profile modifications from dual-LITER

ii) Assessed HHFW heating in deuterium H-modes for advanced scenario applications

iii) Incorporated n=1 RWM/RFA and n=3 EFC control into most operating scenarios

b) FY2009-11 - GOAL: increase f_{NICD} = 65-70%→ 80-90% for $\tau \sim \tau_{CR}$

i) Assess confinement, ELM, thermal profile modifications from LLD-I and LLD-II

ii) Increase NBI-CD using lower density, higher/broader electron temperature from LLD

iii) Use higher power HHFW heating with ELM resilience to increase electron stored energy, bootstrap fraction, and non-inductive current fraction in discharges with elevated q achieved via early H-mode and early strong shaping (see Figure 6.2.3).

iv) Perform high-elongation wall-stabilized plasma operation – FY09 milestone

(1) Conditions: κ up to 2.8, $\tau \geq \tau_{CR}$, low electron density for high NBI-CD fraction, high normalized beta for high bootstrap fraction

(2) Integrate ELM reduction techniques into scenarios – use mid-plane coil RMP, or ELM stabilization from Lithium and ELM destabilization from RMP.

(3) Utilize NBI beta feedback to controllably operate near ideal-wall limit

6.3.3 Longer-term plans for improved plasma sustainment – FY2012-2013

The two major upgrades to NSTX proposed to be operational in the FY2012-2013 time period are:

(1) **2012**: A new centerstack (CS) with:

a. increased toroidal field: 0.55T → 1T

b. increased plasma current: 1MA → 2MA

c. increased pulse duration: 1s → 5s (at full TF)

(2) **2013 (incremental)**: A 2nd NBI system with increased tangency radius for improved NBI current-drive efficiency, current profile control, and increased heating power.

Role of upgraded center-stack in fully non-inductive operation

These upgrades are presently planned to be staged, and the CS upgrade is planned to occur first, in part to enable access to higher toroidal field to more rapidly enable access to higher non-inductive current fraction. Higher toroidal field is advantageous for increasing the non-inductive fraction for several reasons. First, bootstrap fraction $f_{BS} \propto \beta_P$, where the poloidal beta $\beta_P \propto \beta_N q^*$ where β_N is the normalized beta and q* is the kink safety factor. Since $q^* \propto B_T$, f_{BS} can be increased significantly without increasing the drive for pressure-driven instabilities, i.e. without increasing β_N. Or, β_N may be reduced to values further away from the ideal-wall limit without large sacrifices in bootstrap fraction. Second, as described in Chapter 3, the electron thermal confinement is proportional to B_T, so increased toroidal field is projected to increase the electron temperature and increase both the bootstrap fraction and the beam current-drive efficiency. Of course, if the total stored energy does not increase $\propto B_T^2$ as the field is increased, the toroidal beta will decrease and could approach values that are less attractive for next-step ST applications. However, the 2nd NBI would double the available NBI heating power and provide

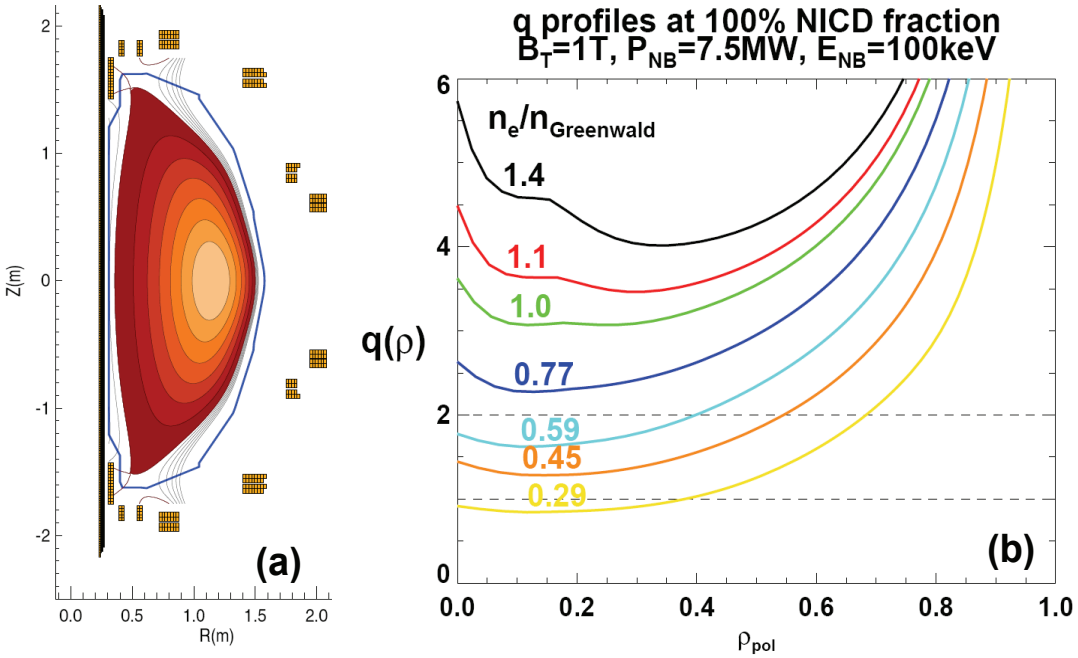

Figure 6.3.3: (a) Plasma equilibrium used in fully non-inductive profile calculations, and (b) q profile variation as the plasma density is varied between $n_e / n_{Greenwald}$ = 0.3 to 1.4 for fully non-inductive scenarios with B_T = 1T (utilizing the CS upgrade) and 7.5MW of injected NBI power using the existing 3 NBI sources.

additional plasma current, enabling recovery of access to high beta at high toroidal field if a single NBI source is insufficient to reach the beta limit at high field.

As shown in Figure 6.3.3a, the proposed new CS capable of high toroidal field = 1T operation supports strongly shaped diverted equilibria with A=1.6, κ=2.7, and δ=0.7. For the equilibrium shown, the divertor coils are designed and operated to generate very large poloidal flux expansion ($|\nabla\psi_p|$ ratio of 20-40) while exhausting the outer SOL flux surfaces onto the outboard divertor where LLD will be located. For the new CS, additional divertor PF coils could prove quite important in controlling and optimizing the plasma exhaust to the divertor targets.

The broadened operating space enabled by a doubling of the toroidal field is very valuable for determining the optimal profiles and other parameters for achieving full non-inductive current drive in next-step STs. A key profile for stability and confinement optimization is the magnetic safety factor profile. As shown in Figure 6.3.3b, with increased toroidal field = 1T, fully non-inductive scenarios can be obtained for a wide range of q profiles with q_{min} ranging from 1 to 4 as the electron density is varied

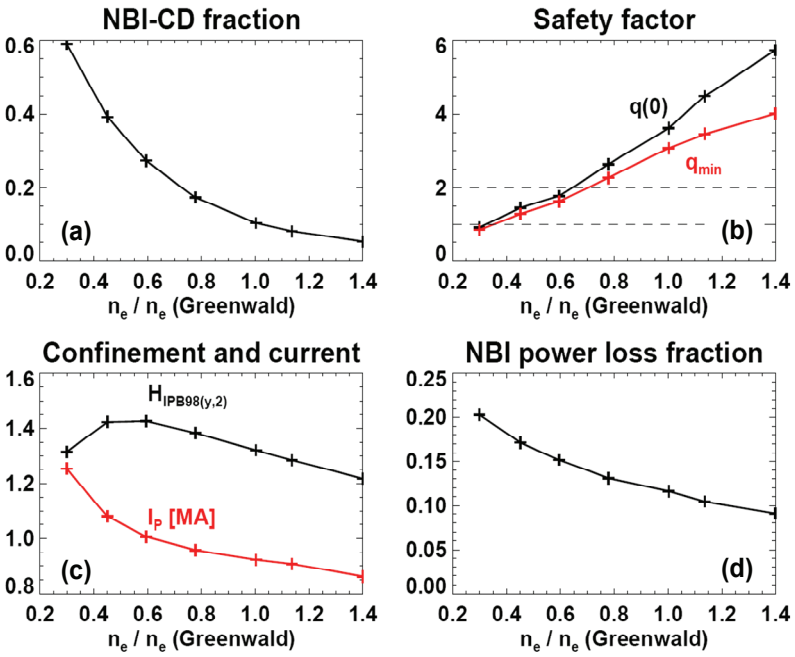

Figure 6.3.4: (a) Fraction of NBI CD, (b) central and minimum q, (c) H-mode confinement multiplier and plasma current, and (d) fraction of NBI power lost as a function of electron density ratio n_e / $n_{Greenwald}$ for the fully non-inductive scenarios of Figure 6.3.3.

from a Greenwald fraction n_e / $n_{Greenwald}$ = 0.3 to 1.4. In these scans, the density is used to control the central NBI-CD efficiency which in turn controls q_{min}. Importantly, access to such a range of q profiles can be achieved at β_N = 4.5-5 which is near the n=1 no-wall limit. These profiles can be achieved using a combination of BS current and NBI current drive using the existing 3 NBI sources operated at 100keV and 7.5MW of total injected power plus an additional 4MW of HHFW heating power. For reference, the density and temperature profiles used in the TRANSP calculations of these profiles are scaled versions of the experimental profiles from discharge 116313 discussed in Figure 6.2.1, and T_i/T_e is held fixed at 1.5. As is evident from the figure, $q_{min} > 1$ is accessible for $n_e / n_{Greenwald} > 0.35$-0.4, and $q_{min} > 3$ is accessible for $n_e / n_{Greenwald} \approx 1$. For these scenarios, $\beta_T \approx 10\%$, and higher β_T could be achieved from higher β_N or from higher current from increased NBI power from the 2nd NBI.

For these fully non-inductive scenarios at higher toroidal field = 1T, a key consideration is the plasma confinement required to support the plasma thermal energy and associated bootstrap current. To absorb most of the injected NBI power (more than 80%) over a wide range of plasma density variation, sufficient plasma current and density must be present. With only 7.5MW of auxiliary heating power from the existing 3 NBI sources, $H_{IPB98(y,2)}$ factors of 1.5-1.7 would be required to support the plasma thermal energy to provide the bootstrap current and NBI-CD to support the equilibrium. These high values are beyond those assumed for next-step STs, and additional auxiliary heating power is required to reduce the required confinement closer to the assumed values. For this reason, an additional 4MW of HHFW

heating power is added to the scenarios above resulting in $H_{IPB98(y,2)}$ values of 1.2-1.4 which are closer to presently achievable experimental values. Since 2MW of HHFW heating power can presently be coupled to NSTX H-mode discharges, the planned antenna upgrade to double the coupled power should provide sufficient margin to supplement the NBI heating power with up to 4MW of HHFW power. As shown in Figure 6.3.4, with this additional heating power, a wide range of NBI-CD fractions = 5 to 60%, q_{min} values = 1 to 4, and I_P = 0.85 to 1.25MA are in principle accessible with at least 80% of the NBI power absorbed without exceeding $H_{IPB98(y,2)}$ = 1.5 which is the H-mode confinement enhancement value assumed for ST-CTF. Should these levels of confinement not be achievable, additional heating power from the 2nd NBI (see Figure 6.3.8 below) could reduce the required $H_{IPB98(y,2)}$ to values less than 1.2, i.e. values achievable in present experiments. Another possibility is to operate at lower plasma current (and β_T) as shown for the TSC simulation of Figure 6.3.9.

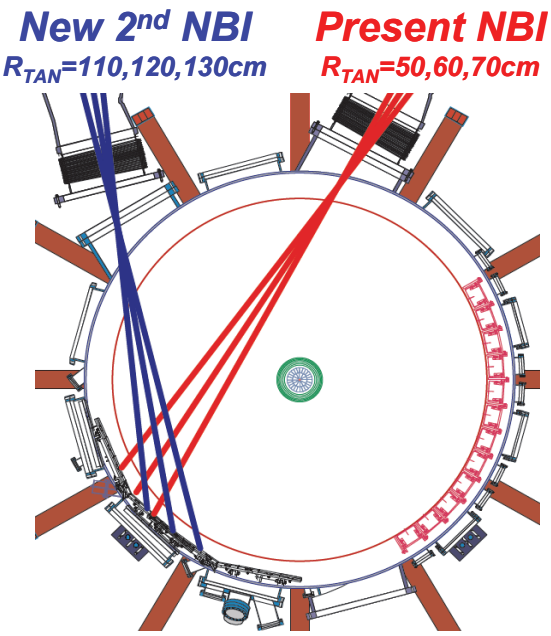

Figure 6.3.5: Injection geometry of present NBI (red) and proposed 2nd NBI (blue) with increased tangency radius of injection.

Role of 2nd NBI in fully non-inductive operation

As shown in Figure 6.3.5, the injection geometry of the proposed 2nd NBI is much more tangential than the present NBI system. The more tangential injection geometry is chosen to provide increased current drive efficiency while also providing for more variability in the driven current profile – ranging from centrally peaked to a profile broader than that obtain with any of the existing sources. As described below, this variability in the NBI-driven current profile can provide a means to modify and control the equilibrium q profile.

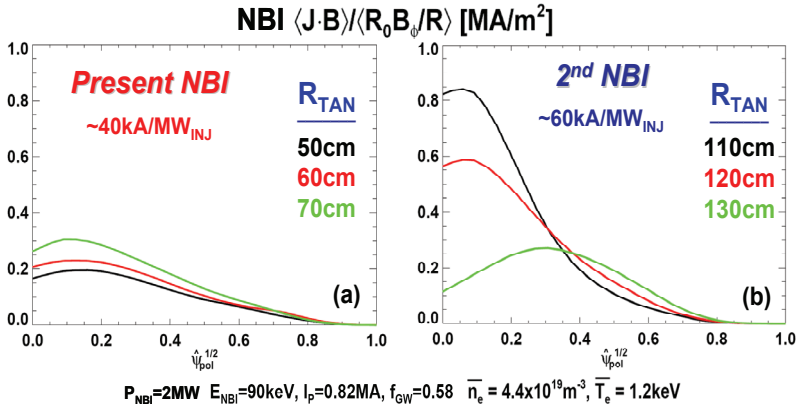

Figure 6.3.6: Comparison of the NBI-CD profiles for (a) the present NBI and (b) the proposed 2nd NBI with increased tangency radius.

As shown in Figure 6.3.6a, for the present NBI injection system, the profile shapes of the NBI-CD depend very little on the tangency radius of the source. The only significant difference among these sources is the 30% lower CD efficiency of the R_{TAN}=50cm source relative to the R_{TAN}=70cm source. In contrast, as shown in Figure 6.3.6b, the 2nd NBI source with increased tangency radius provides up to a factor of 8 variation in driven central current drive, and all three sources offer higher current drive efficiency than the present NBI system by a factor of 1.5 to 2. The combination of the existing and 2nd NBI systems would provide a wide range of possible NBI-CD

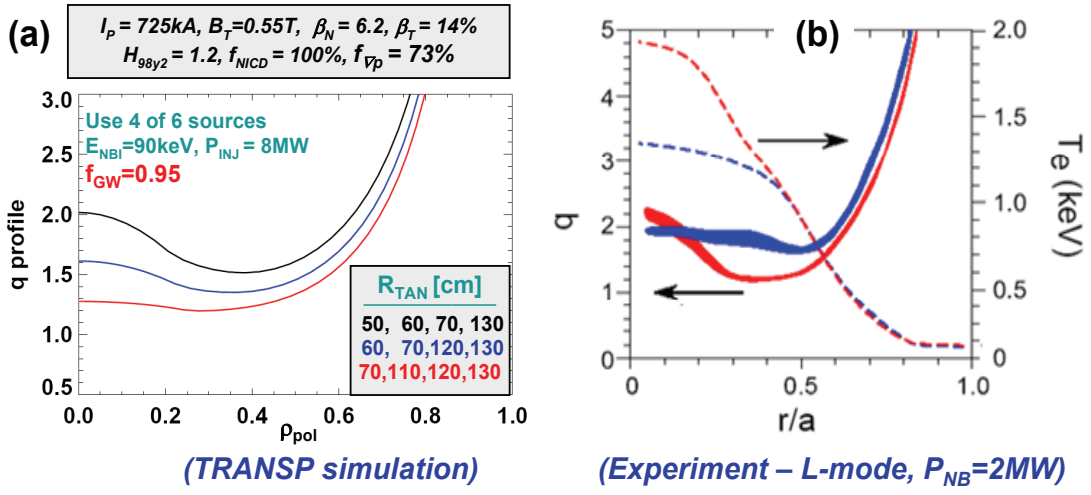

Figure 6.3.7: (a) Simulated q profiles for a mix of present and new NBI sources chosen to vary the degree of magnetic shear reversal while maintaining q_{min} > 1.2, and (b) experimentally observed variation of electron confinement with magnetic shear in L-mode.

profiles and resultant q-profiles while also providing increased heating power to increase the plasma stored energy to increase the bootstrap fraction at confinement and beta values comparable to those presently achieved. Figure 6.3.7a shows that even at the relatively low value of toroidal field of 0.55T of the present CS, fully non-inductive plasmas with q_{min} = 1.2 to 1.5 can be obtained with $\beta_N \approx 6$ and

$H_{IPB98(y,2)}$ = 1.2 by operating at $f_{GW} \approx 1$ – values comparable to those achieved in present experiments. Further, by varying the mix of available sources, the degree of shear reversal can be controlled.

As shown in Figure 6.3.7b, the magnetic shear is an important parameter in determining the electron transport in L-mode, and the influence of magnetic shear on electron transport presumably applies to H-mode scenarios as well. Thus, the q profile control enabled by the combination of the existing and 2nd NBI could provide a means of modifying and possibly controlling core electron transport. Control of the equilibrium q profile using NBI-CD could also be used to control and optimize MHD stability.

As shown in Figure 6.3.8, at higher B_T = 1T and with 4 NBI sources (P_{NB} = 10MW), q profile control with q_{min} = 1.0 to 2.2 is possible by varying the mix of present and new sources in combination with electron density variation. This capability would enable controlled studies of NTM and low-n kink/RWM stability with and without a q=2 surface in the plasma, and as a function of core magnetic shear. This research is highly relevant to next-step STs presently assumed to operate with q_{min} > 2 to avoid low-n NTMs and thereby eliminate the requirement for active control techniques for stabilizing NTMs. Importantly, these results show that the combination of higher toroidal field of the new CS and the additional NBI sources from 2nd NBI should enable the achievement of fully non-inductive scenarios with controllable core safety factor (including q_{min} > 2) with normalized values of plasma density, confinement, and stability achieved in present experiments, namely: $n_e / n_{Greenwald}$ = 0.72 to 0.95, $H_{IPB98(y,2)}$ = 1.1 to 1.2, and β_N=5.1. Fully non-inductive solutions at lower B_{T0} = 0.75T also exist with I_P=1MA, β_T = 16%, β_N = 6.1, $n_e / n_{Greenwald}$ = 0.7, $q_{min} \geq 1.3$, and $H_{IPB98(y,2)}$ =1.25.

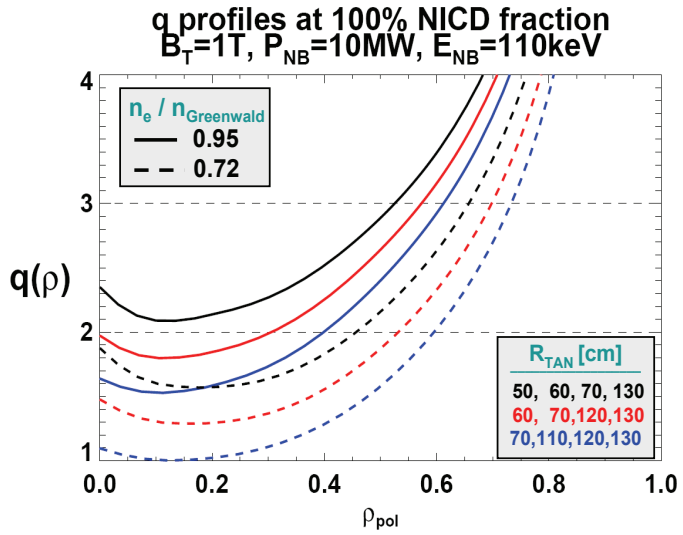

Figure 6.3.8: TRANSP simulations of full NICD q profiles vs. NBI source at B_T=1T, I_P=0.95MA, $n_e / n_{Greenwald}$ =0.72 and 0.95, $H_{IPB98(y,2)}$= 1.2, β_N=5, β_T=10%, P_{NB}=10MW, P_{RF}=4MW

Finally, not only is HHFW heating power projected to be important for achieving fully non-inductive conditions with reduced thermal confinement requirements, but current drive from HHFW is also potentially useful as an on-axis current profile control tool. In particular, the HHFW-driven current density shown in Figure 4.1.1 of Chapter 4 scales to 0.4MW/m^2 at P_{RF}=4MW for the $n_e / n_{Greenwald} = 0.72$ plasma scenario shown in Figure 6.3.8. This RF-driven current density is approximately 50% of the equilibrium current density at the magnetic axis, so HHFW-CD could in principle provide significant additional control of q(0), and therefore of the magnetic shear in the plasma core by raising q(0) from 1.2-1.5 to values above 2.

Pulse-length requirements for current profile equilibration

Sufficient flat-top duration (several current relaxation times) is required to achieve and demonstrate stationary fully-non-inductive current drive. Such a demonstration would significantly increase confidence in extrapolating present understanding and control of non-inductive current drive sources to next-step ST devices. As described above, scenario modeling indicates that full non-inductive operation can most effectively achieved at higher TF (i.e. at least 0.55T and preferably 0.8-1T). Since the proposed scenarios all operate at higher electron temperature than presently achieved in high density H-modes, the current redistribution time is expected to increase by up to a factor of 3 - from approximately 0.3s to up to 1s if the electron temperature doubles.

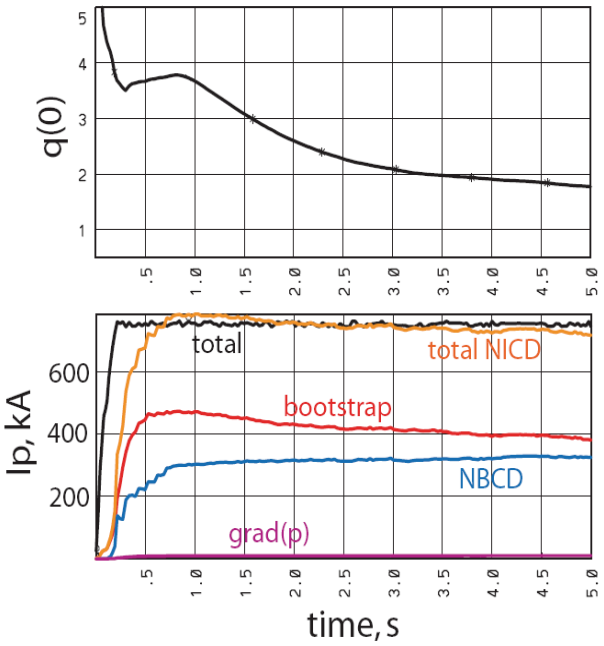

Figure 6.3.9: Preliminary TSC simulations indicating that nearly stationary fully non-inductive 1T, 750kA discharges are possible with upgraded TF and NBI capabilities.

As seen in Figure 6.2.5 above, 2 to 3 current redistribution times are required for the current profile to reach a partially inductively-driven equilibrium, and an additional 2 to 3 current redistribution times are needed to measure the profiles as stationary. Thus, we also expect that toroidal field flat-top duration at least 3 times longer than presently achievable is required to achieve and measure

a stationary fully non-inductive current profile. The upgraded CS is designed to provide a 5s flat-top duration at full TF = 1T and is consistent with this requirement, and could operate for up to 8s at B_T = 0.8T if additional pulse-length is required at high toroidal field.

These simple estimates of the flat-top durations required to approach current profile equilibration with full non-inductive current drive are consistent with time-dependent simulations performed with the TSC code. Shown in Figure 6.3.9 is a TSC simulation result in which a 1T, 750kA fully non-inductive discharge is achieved at near stationary conditions using 6.15MW of absorbed neutral beam power with a Greenwald density fraction = 0.6 and H_{98} confinement factor of 1.15. By t=5s the central q is nearly independent of time with q(0) = 1.8 and li(1) = 0.88. These results are consistent with the TRANSP simulation results of Figure 6.3.3 scaled to lower plasma current and H-mode confinement enhancement.

Additional capabilities needed to support long-pulse operation

Divertor heat flux mitigation

One key area of concern for the upgraded NSTX is the power handling capability of the plasma material interfaces. Recent heat flux scaling studies in NSTX over a limited range of plasma current (700kA to 1MA) indicate a very strong (faster than inverse) narrowing of the divertor heat-flux width as the plasma current is increased. These scalings need to be developed over a much wider parameter range to improve their utility in projecting to future ST devices, but using these scalings, very narrow midplane SOL profile widths (4-6 mm) and high divertor heat-fluxes (10's of MW/m^2) at or beyond ITER values are projected to be possible at higher field and heating power in NSTX. Further, recent results indicate that Li-conditioning of the plasma facing components using evaporated lithium can result in further narrowing of the SOL heat-flux width. Heat flux reduction from enhanced divertor radiation and partial outboard divertor detachment has already been demonstrated on NSTX [20] and has shown to be compatible with good plasma performance in H-mode at high density. Partial detachment can be further tested at higher heat flux and in reduced recycling conditions enabled by the LLD. The compatibility of radiative divertor solutions with reduced recycling and n_e control from LLD is a key question for the NSTX 5 year program.

To provide additional heat-flux reduction tools for NSTX, the enhanced divertor coil set shown in Figure 6.3.3 proposed for the upgraded CS would improved strike point control, enable strike point sweeping, and enable increased outboard divertor flux expansion as proposed for the "X-divertor" [21]. Finally, divertor heat fluxes in the range of 10MW/m^2 exhausted onto the LLD-I (cooled between shots) are expected to cause the LLD surface temperature to increase at a rate of 0.35°C/ms to 0.5°C/ms. Thus, the liquid lithium would reach evaporation temperatures on time-scales of order 1s and active cooling of the LLD would be required for compatibility of the LLD with long-pulse (5s) operation. It should also be noted that for similar heat fluxes, graphite PFC temperatures in the divertor are projected to reach an NSTX administrative limit of 1200°C within 2-3 seconds. Thus, for very high heat fluxes, active divertor cooling may be required for long-pulse operation independent of the type of divertor used in NSTX.

ELM and impurity control

Another potential concern is the impact of high transient heat loads from Edge Localized Modes (ELMs). While ELMs may not be problematic for the NSTX divertor, they could severely limit the lifetime of the divertor of ST-CTF. ELMs are also considered a major problem for ITER, and both pellet pacing and resonant magnetic perturbations (RMPs) are being considered to mitigate ELMs to limit the ELM energy density loss (to < 0.5MJ/m^2) to avoid ablation/melting of C/metal divertor PFCs. Recognizing the importance of ELM mitigation to future ST devices and ITER, a high-n RMP coil set is part of the NSTX 5 year upgrade plan. As discussed in Chapter 2 on MHD stability, these non-axisymmetric control coils (NCC) also have a wide range of additional applications including control of rotation, error-fields, and resistive wall modes.

As described in Chapter 5, an important recent result from NSTX is that the existing mid-plane RMP coils (RWM/EF coils) have been shown to *de-stabilize* ELMs rather than stabilize them, despite having satisfied the Chirikov > 1 criterion over most of the pedestal width as has been observed to be required for ELM mitigation in experiments on DIII-D [22]. The mechanisms for the observed ELM destabilization in NSTX plasmas are not yet understood. NSTX does not observe density pump-out during RMP as observed in other experiments, perhaps due to the lack of active pumping. One possible explanation of these results is that rotational shielding of the applied RMP fields may be limiting the degree of ergodization in NSTX RMP experiments, while the 3D RMP magnetic field perturbation modifies the

plasma rotation and/or the neoclassical or turbulent transport in the pedestal which in turn modifies the pedestal stability.

Despite the lack of success of suppressing ELMs with RMP fields in NSTX, Li-conditioning of the PFCs has succeeded in eliminating ELMs completely resulting in ELM-free H-mode. While this leads to significant and beneficial increases in thermal confinement, impurity accumulation and high radiation fractions are also observed in such conditions. Importantly, ELM destabilization from the mid-plane RMP coils has successfully triggered Type-I ELMs in these conditions and has reduced the impurity accumulation by a factor of two in initial experiments. Additional optimization is needed to reduce the ELM size and radiation levels further, but overall, the combination of Lithium with RMP fields appear very promising as a means of controlling ELMs and impurity accumulation. A significant issue with the present RMP coil set is the lack of poloidal mode number spectral control and the resultant inability to strongly resonantly interact with the plasma edge at higher edge q values. Since the impact of RMPs on edge transport and stability remains poorly understood, and because a high degree of spectral flexibility is important to allow controlled RMP experiments, the NCC coil set shown in Figure 6.3.10 is high priority in the NSTX 5 year plan with incremental funding. Importantly, this proposed coil set in combination with the existing coil set would have a configuration very similar to that proposed for ITER, i.e. with coils above, at, and below the midplane with high-n (n > 3) capability. The high-n (up to n=6) NCC system would be a unique and important capability for understanding RMP and MHD physics in general. Further, this capability could be important for localizing field perturbations to the plasma edge to minimize core flow damping to aid rotational stabilization of resistive wall modes for stable long-pulse operation at high β_N.

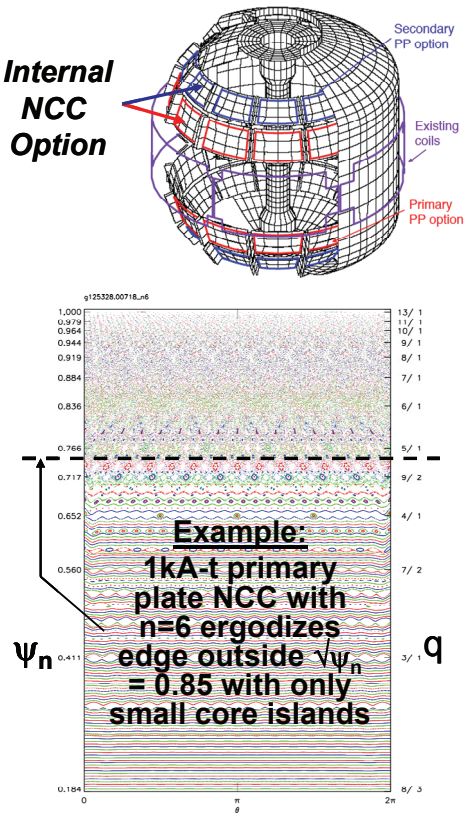

Figure 6.3.10: (top) NCC coils proposed for NSTX, (bottom) example of vacuum field calculation of localized ergodization of edge using n=6 RMP.

1) Plans for assessing impact of major upgrades on plasma performance and sustainment

a) FY2012

i) Assess impact of higher A on vertical stability and n > 0 no-wall and ideal-wall stability limits. Determine if sufficient power is available to reach n > 0 stability limits at higher B_T.

ii) Assess impact of higher B_T on energy confinement in general, and electron confinement in particular, and the impact of confinement on plasma sustainment.

iii) Assess impact of higher B_T on non-inductive current drive sources

(1) Assess impact of higher B_T on bootstrap fraction through confinement modifications

(2) Assess impact of higher B_T on NBI-CD efficiency as a function of T_e

(3) Assess impact of higher B_T on fast-ion-driven instabilities and possible redistribution of fast-ions and NBI-CD.

(4) Implement real-time MSE diagnostic for future current profile control

iv) Assess impact of higher B_T and I_P on SOL and divertor heat-flux widths

v) Assess impact of longer pulse-length on divertor temperature evolution, and develop operating scenarios that minimize peak heat flux as required.

vi) Assess impact of NCC coils (incremental) on pedestal stability in long-pulse discharges.

b) FY2013

i) Assess HHFW coupling, heating, and CD at higher B_T

(1) Vary central HHFW-CD to vary q(0), assess impact on confinement and MHD stability

(2) Using real-time MSE, implement and assess algorithms for HHFW-based q(0) control

ii) Assess impact of NCC coils (incremental) on rotation damping and SOL heat flux widths in sustained conditions.

The additional research plans below assume the 2nd NBI is available during FY2013 (incremental):

iii) Assess impact of more tangential injection on fast-ion distribution function and on Alfven eigenmode stability and resultant impact on driven current profile. Assess predicted vs. measured power deposition and current drive profiles from new NBI sources.

iv) Assess impact of higher power and lower collisionality on SOL and divertor heat-flux widths and impact of divertor performance on plasma sustainment – for example impurity influx and accumulation.

v) Assess impact of higher power and/or more tangential injection (and possible fast-ion losses) on divertor temperature evolution, and develop operating scenarios that minimize peak heat flux as required.

vi) Vary mix of NBI sources to vary NBI-CD profile to modify q profile, and assess impact of global stability and confinement properties

(1) Using real-time MSE, implement and assess algorithms for NBI-based J profile control

2009 – 2013 Timeline for Plasma Current Sustainment and Control Research

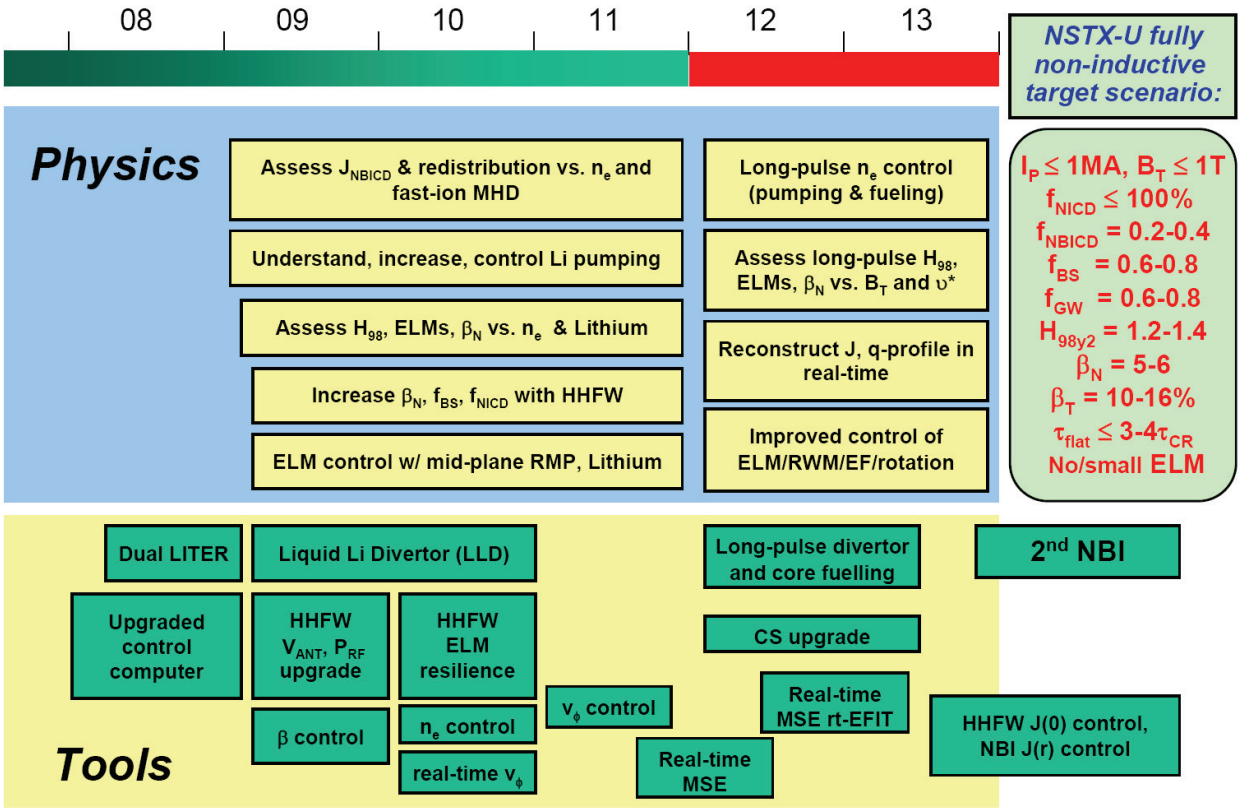

References (for Plasma Sustainment)

[1] Y.-K. M. Peng, et al., Plasma Phys. Control. Fusion **47** (2005) B263–B283

[2] J.E. Menard, et al., PPPL Report 4252

[3] G. Taylor, et al., Phys. Plasmas **11**, (2004) 4733

[4] S.J. Diem, et al., PPPL Report 4307

[5] M. Murakami, et al., Phys. Plasmas **13**, 056106 (2006)

[6] C.D. Challis, et al., EFDA Report EFD-C(07)03/29

[7] M.P. Gryaznevich, et al., EFDA Report EFD-C(07)03/41

[8] S.A. Sabbagh, et al., Nucl. Fusion **46**, (2006) 635–644

[9] A.M. Garofalo, et al., Phys. Rev. Lett. **89**, (2002) 235001

[10] D.A. Gates, et al., Nucl. Fusion **47**, (2007) 1376–1382

[11] J.E. Menard, et al., Nucl. Fusion **47**, (2007) S645–S657

[12] J.E. Menard, et al., Phys. Rev. Lett. **97**, 095002 (2006)

[13] J.E. Menard, et al. Nucl. Fusion **45**, (2005) 539

[14] D.A. Gates, et al., Nucl. Fusion **46**, (2006) S22–S28

[15] J.E. Menard, et al., APS-DPP 2007, Invited talk UI1.00001

[16] H.W. Kugel, et al., Phys. Plasmas 15, 056118 (2008)

[17] F. M. Levinton, et al., Phys. Plasmas **14**, 056119 (2007)

[18] R. Majeski, Phys. Rev. Lett. **97,** 075002 (2006)

[19] C.E. Kessel, et al., Phys. Plasmas **13**, 056108 (2006)

[20] V.A. Soukhanovskii, et al., Journal of Nuclear Materials, Volumes 363-365, 432-436 (2007)

[21] M. Kotschenreuther, et al., Phys. Plasmas **14**, 072502 (2007)

[22] T.E. Evans, et al., Phys. Rev. Lett. **92,** 235003 (2004)

6.4 Plasma start-up and ramp-up results and plans

The Spherical Torus (ST) is capable of simultaneous operation at high beta and high bootstrap current fraction. These advantages of the ST configuration arise as a result of its small aspect ratio. At the low aspect ratios needed for an ST reactor, elimination of the central solenoid is necessary. Thus current generation methods that do not rely on the central solenoid are necessary for the viability of the ST concept. Elimination of the central solenoid could also lead to a more compact tokamak. Thus ST-based fusion systems including the CTF (Component Test Facility) and power plant designs (e.g., ARIES-ST) assume complete elimination of the ohmic solenoid. The investigation of plasma start-up without the ohmic solenoid is a major component of the NSTX research program. NSTX is exploring the technique known as Coaxial Helicity Injection (CHI) [1] and Outer Poloidal Field Start-up [2] as methods to produce the initial plasma and sufficient toroidal plasma current to allow other methods of non-inductive current drive and sustainment to be applied. Other new methods such as Plasma Gun Injection [3] will also be studied during the FY 2009 to 2013 period. Of the three US major magnetic fusion facilities (DIII-D, NSTX, C-Mod), at the present time NSTX is the only one actively conducting OH-solenoid-free start-up research. The goal of solenoid-free startup research in NSTX is to first generate high current discharges that do not rely on the central solenoid and then to ramp these up non-inductively to currents >800 kA using NBI and RF with minimal reliance on induction from the central solenoid.

6.4.1 Coaxial Helicity Injection

The CHI concept is an outgrowth of the spheromak research [4]. It has also been tried on DIII-D [5]. A number of smaller helicity injection experiments were performed with some success prior to introducing it on NSTX [6-9]. More recently, the HIT-II device has unambiguously demonstrated plasma start-up using this method [10]. The method has now also successfully produced 160kA of closed flux current in NSTX, which is a world record for non-inductively generated closed flux current [11,12]. As part of the proposed center stack upgrade to NSTX, the toroidal field in NSTX would be nearly doubled from present values. As described later, this now gives NSTX the potential to produce more than 500kA of CHI produced closed flux current, a level at which the realization for non-inductive startup, ramp-up and sustainment become much easier. The CHI research on NSTX has benefited greatly from a close

collaboration with the HIT-II experiment at the University of Washington. The CHI near term research goal is to improve the coupling of the CHI produced current to induction from the central solenoid and beyond that to other non inductive current drive methods.

CHI is a promising candidate for non-inductive current initiation and has, in addition, the potential to drive edge current during the sustained phase of a discharge for the purpose of controlling the edge current profile to improve plasma stability limits and to optimize the bootstrap current fraction. Other possible benefits include inducing edge plasma rotation for transport barrier sustainment and controlling edge SOL flows. The development of these methods would improve the prospects of the ST as a fusion reactor.

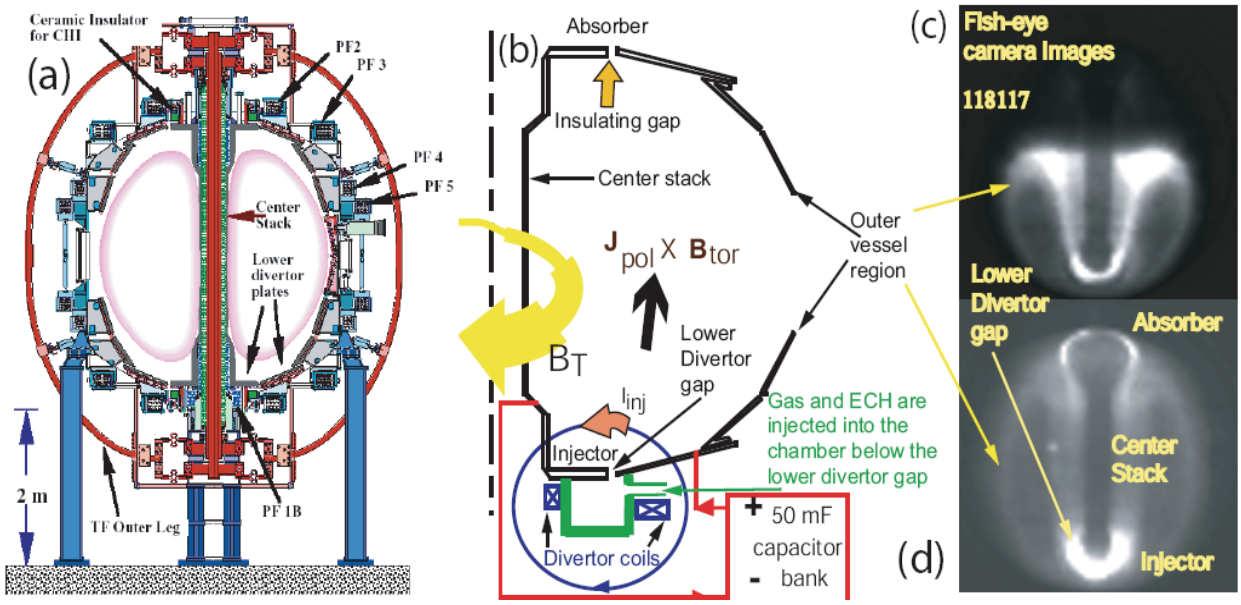

Figure 6.4.1: (a) The NSTX machine layout showing the location of the toroidal insulator and external poloidal field coils. Shown also are (b) the NSTX machine components used for CHI startup in NSTX and fast camera fish eye images showing (c) discharge evolution from near the injector region and (d) later during the discharge. Both gas and 18 GHz microwave power are injected in to a 100 Liter toroidal cavity beneath the lower divertor plates. The gas, which is ionized by the microwaves, emerges from the gap between the lower divertor plates, which eases the requirements for breakdown when the main capacitor bank discharge is initiated.

An important advantage of CHI start-up is that it could be used for closed flux plasma generation without any time variations in the PF coil currents as demonstrated on HIT-II [13]. Therefore, it is compatible

with future reactor system that would rely on superconducting PF coils, and PF coils located far away from the plasma.

CHI implementation on NSTX - In order to accommodate CHI, the stainless steel vacuum vessel (nominal major radius 0.85 m, volume 30 m^3) has separate inner and outer sections, electrically isolated from each other by toroidal ceramic rings at the top and bottom which also act as vacuum seals. An alternate way to implement it is to insulate one of the lower divertor plates from the rest of the vessel as was done in D-III-D. This would avoid the need for a vacuum insulator. The inner divertor plate, which is part of the center stack assembly, is then electrically separated from the outer divertor plate, which is attached to the outer vessel. This is illustrated in Figure 6.4.1. For CHI, the poloidal field coils located beneath the lower insulated gap are used to produce poloidal flux connecting the lower inner and outer divertor plates, as indicated qualitatively by the circle in Figure 6.4.1b. When a small amount of deuterium gas is introduced into the chamber below the lower divertor plates and a voltage (typically 1 – 2 kV) is applied between the plates, a discharge forms with current flowing in the plasma from the outer divertor plate to the inner lower divertor plate, as shown by the arrow in Figure 6.4.1b. In the presence of a toroidal field, the plasma current, which essentially flows along field lines, develops a toroidal component. The bright region at the top of Figure 6.4.1c is the top of the CHI plasma that has extended to approximately the middle of the vessel at a time during the discharge when the plasma current is below the peak value. As the plasma current increases to near the peak value, the discharge further elongates vertically to fill the vessel as shown in Figure 6.4.1d. The bright ring shaped region at the top of this image is referred to as an absorber arc, a condition when part of the injector current bridges the upper divertor gap. We refer to the lower gap connected by the poloidal field as the injector and the complementary upper gap as the absorber because when voltage is applied toroidal flux flows out of the injector and into the absorber.

The toroidal plasma current produced by CHI initially flows on open field lines joining the electrodes. In order to produce toroidal plasma current on closed flux surfaces magnetic reconnection must occur. In steady state, this reconnection depends on the development of some form of non-axisymmetric plasma perturbation. In transient CHI, the initial poloidal field magnitude is chosen such that the plasma carrying the injected current rapidly expands into the chamber. When the injected current is rapidly decreased,

magnetic reconnection occurs near the injection electrodes, with the toroidal plasma current forming closed flux surfaces. The method of transient CHI has now been successfully used on NSTX producing an unambiguous demonstration of closed-flux current generation without the use of the central solenoid.

Transient CHI Startup- CHI can be applied in two ways. In both methods the toroidal plasma current produced by CHI initially flows on open field lines joining the electrodes. In order to produce toroidal plasma current on closed flux surfaces magnetic reconnection must occur. In the first approach referred to as *steady state* or *driven* CHI, closed flux current generation relies on the development of some form of non-axisymmetric plasma perturbation. This mode of CHI operation, in which the injector circuit is continuously driven for a time longer than the timescale for resistive decay of the toroidal current ($t_{pulse} > \tau_{L/R}$) was initially studied in the early CHI experiments in NSTX [14, 15, 16]. However, for the purpose of initial plasma startup it was found in the HIT-II ST that a new mode of CHI operation in an ST, referred to as *transient* CHI [10], which involves only axisymmetric magnetic reconnection works very well and produces useful closed flux equilibrium. In transient CHI, the initial poloidal field configuration is chosen such that the plasma carrying the injected current rapidly expands into the chamber. When the injected current is rapidly decreased, magnetic reconnection occurs near the injection electrodes, with the toroidal plasma current forming closed flux surfaces. The method of transient CHI has now been successfully used on NSTX producing an unambiguous demonstration of closed-flux current generation without the use of the central solenoid [17]. The transient CHI method is therefore now being pursued as the preferred CHI method to start the NSTX discharge without the use of the solenoid.

There are two objectives for CHI research on NSTX. The primary objective is to start-up the NSTX plasma using CHI and to hand it off initially to inductive operation and then later to a non-inductive current drive system. The second objective is to provide edge current drive during sustained non-inductive operation, for the purpose of controlling the edge current profile and to modify the edge SOL flows.

For transient CHI, a 5-45 mF capacitor bank was used at up to 1.75kV to provide the injector current. The present operating condition for CHI in NSTX uses the inner vessel and inner divertor plates as the cathode while the outer divertor plates and vessel are the anode. The operational sequence for CHI

involves first energizing the toroidal field coils and the CHI injector coils to produce the desired flux conditions in the injector region. The CHI voltage is then applied to the inner and outer divertor plates and a pre-programmed amount of gas and 10kW of electron cyclotron waves at 18GHz are injected in an injector cavity below the lower divertor plates. This condition ensures that there is adequate energy in the capacitor bank for ionization and heating of the injected gas. The resulting current initially flows along helical magnetic field lines connecting the lower divertor plates. The large ratio of the applied toroidal field to the poloidal field causes the current in the plasma to develop a strong toroidal component, the beginning of the desired toroidal plasma current generation. If the injector current exceeds a threshold value, known as the bubble burst condition, the resulting ΔB_{tor}^2, ($J_{pol} \times B_{tor}$), stress across the current layer exceeds the field-line tension of the injector flux causing the helicity and plasma in the lower divertor region to expand into the main torus chamber. The initial poloidal field configuration is chosen such that the plasma rapidly expands into the chamber. When the injected current is then rapidly decreased, magnetic reconnection occurs near the injection electrodes, with the toroidal plasma current forming closed flux surfaces.

In Figure 6.4.2, we show traces for the toroidal plasma current, the injector current and fast camera images at two different times during the discharge. Note that the generated toroidal plasma current is about sixty times the injector current. The CHI capacitor bank discharge is initiated at 5ms. In these experiments the discharge rapidly grows to fill the vessel within about 2ms, then starting at about 9ms the discharge begins to detach from the injector electrodes. At 11ms, the injector current is zero and about 60kA of plasma current is still present. Note that at 13ms, the ring shaped plasma is clearly disconnected from both the injector and the upper divertor plate regions. As time progresses, the large bore plasma that fills the vessel gradually shrinks in size and after about t = 14ms, it evolves into a small diameter plasma ring, as seen in the 15ms time frame image. The formation of closed flux regions is clearly seen in the camera frames corresponding to 11ms and beyond as expected from a decaying closed magnetic flux configuration. For these discharges, circuit calculations show that only about 7kJ of capacitor bank energy is expended to generate 60kA of closed flux current. Electron pressure and temperature profiles from Thomson scattering show that profiles at later times are less hollow than at earlier times. This is consistent with the CHI startup process, since initially CHI drives current in the edge. After reconnection in the injector region, one expects the current profile to flatten, which should result in the profiles

becoming less hollow. The evolution of a hollow pressure profile into a peaked pressure profile is shown in Fig. 6.4.2c. The measured electron temperatures of about 20eV, combined with a plasma inductance of about 0.5 – 1μH, should result in an e-folding current decay time on the order of about 8ms, which is consistent with the observed current persistence time after the injector current has been reduced to zero.

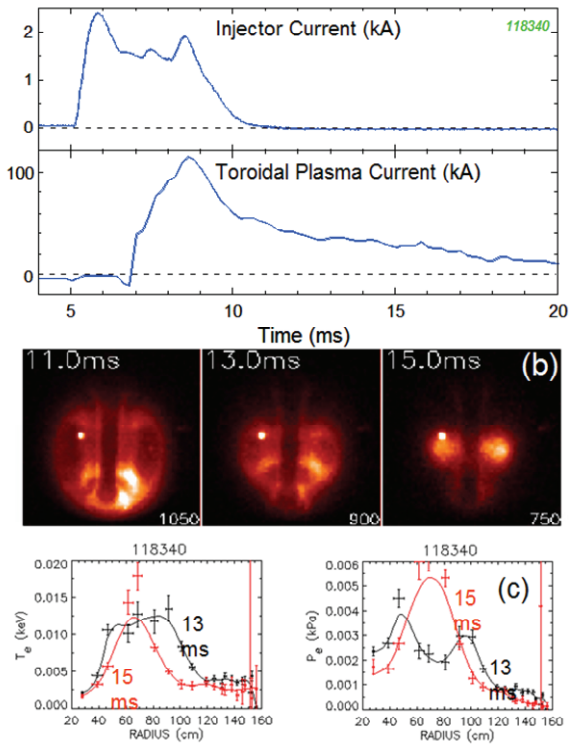

Figure 6.4.2: Shown are (a) Injector and plasma current traces (b) fast camera images and (c) the electron density and electron pressure profiles, at 13 and 15ms from a CHI discharge in NSTX. In this discharge about 2kA of injector current produces 120kA of toroidal current resulting in a current multiplication of 60. The best attained current multiplication (not shown here) was 70. During these discharges, the NSTX CS was disconnected from its power supply. The small bright glow is light from a tungsten filament. The images at 11 and 13ms show an elongated dark region, which is surrounded by a brighter region, like usual tokamak photos. It is useful to note that an absorber arc has not been produced in this discharge.

Equilibrium reconstructions from discharge 120874 are shown in Figure 6.4.3. The experimentally measured poloidal magnetic field, from 40 sensors, and poloidal flux, from 44 flux loops, are used in the computation of the Grad-Shafranov plasma equilibrium. While equilibrium reconstructions show the presence of closed flux for lower current discharges, such as for example, the data shown in Figure 6.4.2, equilibrium reconstructions for the higher current discharges such as for shot 120874, are much more robust and result in residuals similar to that in conventional inductive discharges. The χ^2, which is a measure of the residual error, for the fit shown in Figure 6.4.3 is 50. At the time I_{inj} is reduced to zero this discharge has 150kA of current, After t = 9ms, there is no I_{inj}, therefore there are no open field line currents. The only plausible explanation for the decaying current magnitude from 150kA to 70kA at 12ms is that it must result from decaying closed flux equilibrium, which is consistent with the equilibrium reconstructions. The LRDFIT Grad-Shafranov equilibrium code, developed by J. Menard, which is now in routine use for NSTX

discharges, is used for these reconstructions. The code uses a circuit equation model of the plasma, vessel, and passive plate currents to better constrain the equilibrium fits at low I_p.

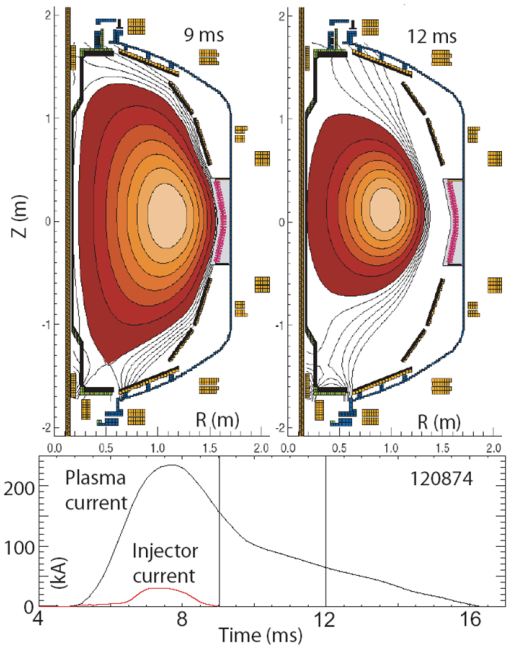

Figure 6.4.3: Equilibrium reconstructions show the shape evolution of the CHI produced plasma in response to decaying current, which is further evidence of decoupling from the injector leaving behind an inductively decaying plasma. In this discharge the increase in I_{inj} around 7.5ms is due to the presence of an absorber arc. Overdriving the injector by using a larger capacitor bank (45mF, charged to 1.8kV) caused a large amount of unused capacitor bank energy to be dissipated as an absorber arc, which probably contributed to an increase in the resistivity of these yet unoptimized discharges.

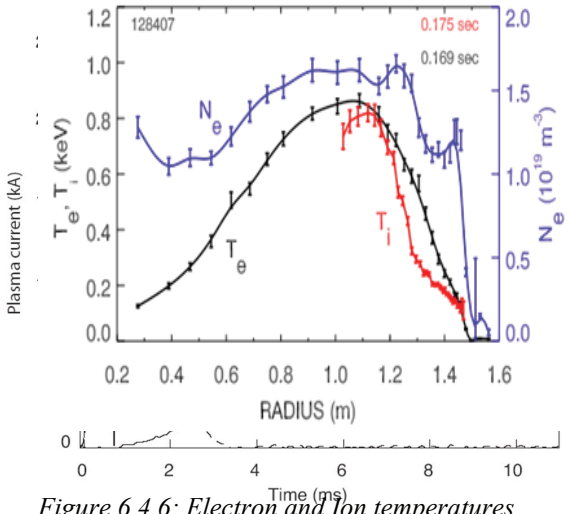

Figure 6.4.6: Electron and Ion temperatures and the density profile of a CHI started discharge. The vertical dashed line shows the time at which the CHI injector current is reduced to zero. CHI current persistence beyond this time is due to the existence of a closed flux equilibrium. It is this closed flux plasma that is inductively driven in shot 30228. For comparison, an inductive only discharge, using the central solenoid, under identical pre-programmed loop voltage time history (total 30 mV s consumed) is also shown (shot 25999).

Figure 6.4.4: The dashed trace is a CHI only discharge. The vertical dashed line shows the time at which the CHI injector current is reduced to zero. profiles are during the H-mode phase.

A result of particular importance for the extrapolation of this method to future machines is that the ratio of the generated plasma current to the injector current exceeds 60 for NSTX. This is an order of magnitude larger than the previous results on HIT-II. Experiments on the HIT-II device have shown that CHI discharges couple to and outperform inductive-only discharges, an example of which is shown in Figure 6.4.4.

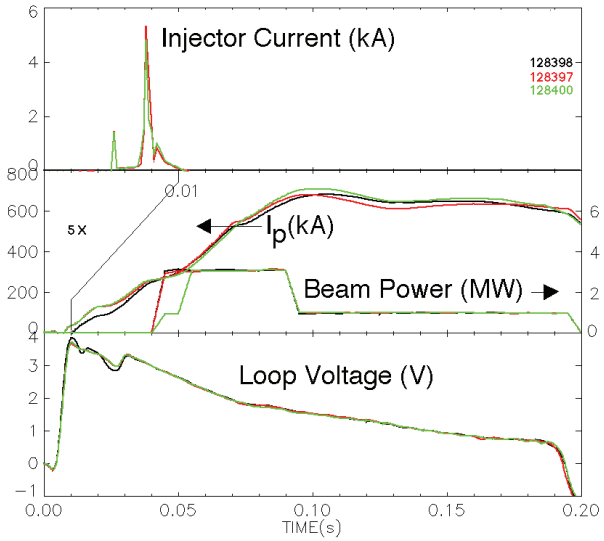

Fig. 6.4.5: Comparison of CHI initiated plasma (green and red curves) with an Ohmic initiated plasma (black curves). Note the expanded time in the top frame. All discharges used the same Ohmic coil current programming.

The Ohmic transformer has been applied in order to provide current drive to sustain and increase the current in CHI initiated discharges on NSTX. Fig. 6.4.5 compares discharges initiated with and without CHI and ramped up to over 600kA using the same ohmic transformer current programming and neutral beam injection heating. CHI initiated discharges can transition into H-Mode, reach electron temperatures of 800eV and have low inductance preferred for high-performance NSTX discharges. Figure 6.4.6 shows the electron density (n_e), electron temperature (T_e) and ion temperature (T_i) profiles for a CHI-initiated, neutral-beam-heated discharge after the transition into H-mode. However, the CHI discharges did not show the flux savings that was seen on HIT-II. The lack of flux savings is probably due to the influx of impurities with the CHI initiation. Earlier attempts to add the ohmic drive to CHI initiated discharge resulted in no increase in I_p, but there was a significant increase in the O-II emission measured by a filter scope [17]. It was not until further conditioning was performed in the form of D_2 glow discharge cleaning (GDC) and electrode discharge conditioning that the plasma current was increased by the OH. Further evidence for the need to condition the walls and/or divertor plates is shown in Figure 6.4.7. Shots taken with 1, 2, and 3 capacitor banks in the CHI system differed primarily in the intensity of the low Z impurity emission and increased radiation measured by a bolometer viewing the injector region with only modest changes in the plasma current. The need for excellent vacuum conditions in order to successfully couple the CHI discharge to Ohmic drive was also found on HIT-II.

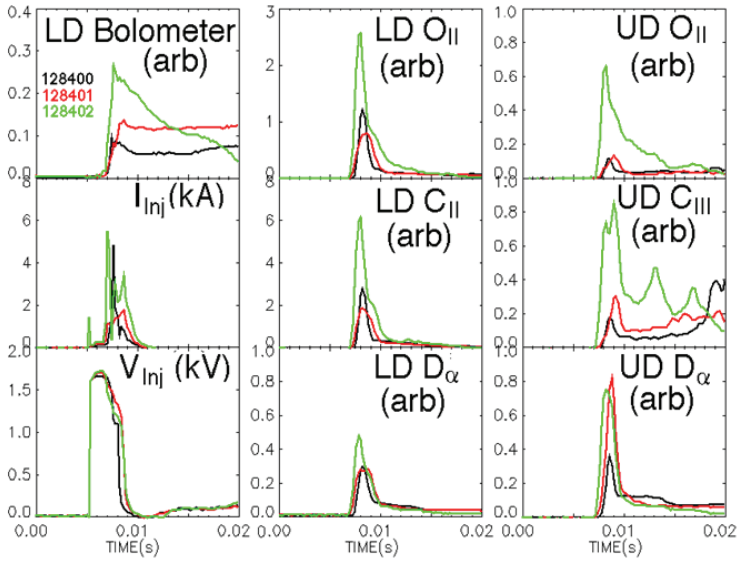

Figure 6.4.7: Discharges with larger capacitor power supplies show increased levels of line radiation and radiated power. Shot 128400 (5 mF bank), 128401 (10 mF), 128402 (15 mF).

Improvements for CHI research

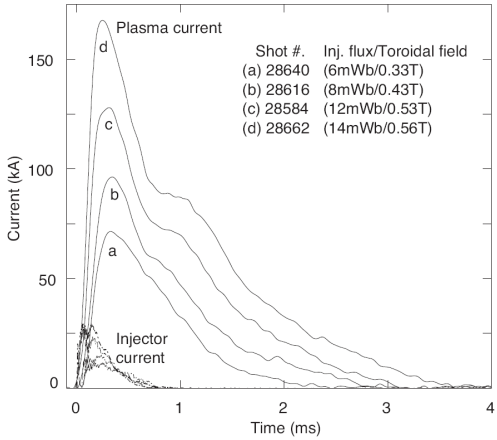

Figure 6.4.8: The amount of useful closed flux plasma current increases with the injector flux. The capacitor bank charge voltages for discharges (a) to (d) are 2.5, 2.7, 3.4 and 3.9 kV respectively. Note that the toroidal field is also increased as the injector flux is increased.

1. ECH Heating of CHI Produced discharges:

Results from the HIT-II experiment show that CHI produced discharges couple to induction only if the power radiated by the decaying CHI discharge is less than the input power from ohmic heating. At an applied loop voltage of about 3V, and at 100kA of plasma current, the ohmic input power is about 300kW. Present CHI discharges are observed to have an electron temperature in the range of 10 to 20eV at the start of the current decay phase. The radiated power from the best discharges is probably about 300kW. Because of the decreased sensitivity of the NSTX bolometers to emission below 20eV, the radiated power cannot be accurately estimated. During 2011, a 350kW ECH system is expected to be

available on NSTX. The ECH system will be used to increase the temperature of the CHI target to improve coupling to induction and to other non-inductive current drive methods.

1. *Higher CHI voltage capability:*

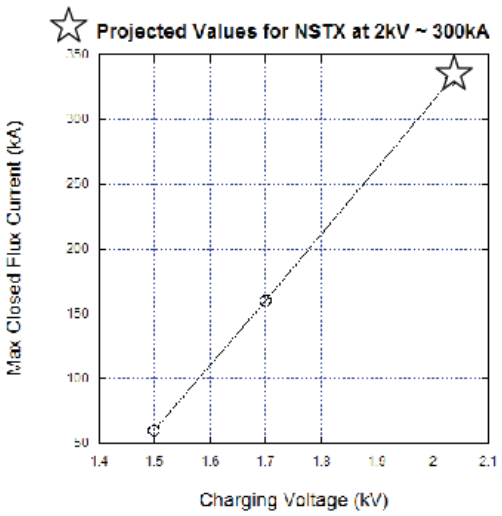

Figure 6.4.9: Projected closed flux current at a capacitor bank charging voltage of 2kV

Results from the HIT-II experiments show that by optimizing the injector voltage, injector flux and toroidal field, the extent of closed flux current can be increased. To increase the closed flux current more injector flux is needed. To reduce the injector current at higher levels of injector flux, the toroidal field needs to be increased. At higher toroidal field, the injector voltage needs to be increased. As a result of such an optimization, the magnitude of closed flux current in HIT-II was increased to 100kA. Figure 6.4.8 shows the results of this optimization.

At present in NSTX, such an optimization scan has not been conducted. At a capacitor bank charging voltage of 1.5kV used during FY 2005, 60kA of closed flux current was achieved. At 1.7kV used during FY 2006-8, 160kA was obtained. As indicated by Figure 6.4.9, at a capacitor bank charging voltage of 2kV closed flux current magnitude of 300kA should be possible. If the voltage could be increased to 2.5kV even higher levels of current should be attainable. If the lower divertor plates could be insulated from the rest of the vessel (similar to the ring electrode that was used on DIII-D), then it should be possible to bias the inner and outer vessel components with respect to this plate, which would allow the injector voltage to be increased to 4kV while maintaining the inner vessel voltage at 2kV. The present voltage snubbing system on the CHI system (the Metal Oxide Varistors) begins to significantly conduct at a voltage of 1.7kV. In order to extend the voltage to the full 2kV, new MOVs with a higher voltage rating are required. This upgrade is planned during 2009-10. In preparation for this, during the 2007 maintenance break, the CHI voltage monitors were improved to better asses the magnitude of the injector voltage transients.

3. Absorber field-null control

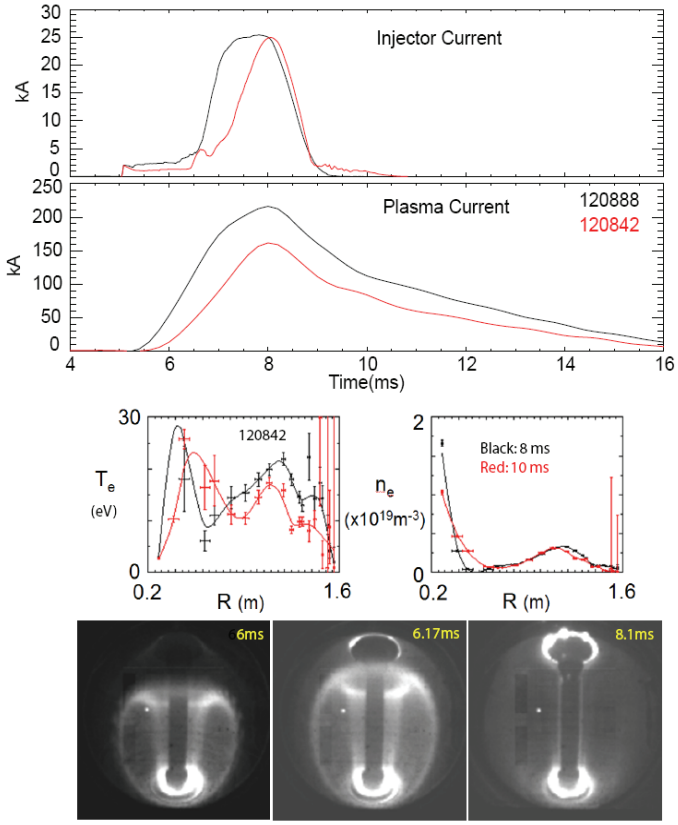

Figure 6.4.10: A discharge (120888) in which about 160 kA of persisting closed flux current is present after the injector current is reduced to zero. A lower current discharge (120842) is also shown along with electron temperature and electron density profiles at 8 and 10 ms. Shown are the injector current, the plasma current, Thomson scattering data (for 120842) and fast camera images for discharge 120888, which show the development of an absorber arc at 6.17 ms. The Absorber arc is seen by the bright visible ring that is seen in the absorber region. The arc can be seen intensifying at 8.1 ms. For comparison, note that the images from Figure 6.4.2 do not show evidence for such a visible light emission in the upper divertor gap.

During CHI discharge initiation, the injected current flows along field lines connected to the lower divertor electrodes. As the magnitude of the injected current increases and the plasma grows to fill the vessel, an ionized region begins to form in the upper divertor region. Because of the presence of some poloidal magnetic field in this region (due to fringing fields from the PF5 and PF3U coils), these stray fields provide a conducting path between the upper divertor plates. If the impedance of this path becomes sufficiently low, such as when an ionized plasma front reaches this region due to an elongated plasma, then an alternate current path can develop along the upper divertor region. This is known as an absorber arc. An example of such an arc is shown in Figure 6.4.10. In NSTX, discharges with no absorber arcs typically draw about 2 – 4kA of injector current. Once the absorber arc initiates, the injector current increases to above 15kA, the maximum level dependent on the size of the capacitor bank. This additional arc current serves no useful purpose and could increase the impurity content in the CHI discharge. On HIT-II, the absorber arcs are minimized by providing a region of poloidal field null in the absorber region. Absorber field control is very effective in minimizing or eliminating absorber arcs in

HIT-II. In preparation for this possibility two new absorber poloidal field coils were installed in NSTX. These coils can be driven using the same power supplies used to drive the Resistive Wall Mode coils in NSTX. Power feed cables from the CHI absorber coils to the RWM power supplies will be installed during the 2008 outage and the plasma control system revised to control these coils to provide a region of poloidal field null in the absorber region during the transient CHI discharge phase.

4. Staged capacitor bank operation

The CHI power supply consists of up to ten capacitors, each 5mF in size. Any number of these can be connected in parallel and discharged using a single ignitron. Adding two more ignitron switches that would allow two or three ganged up capacitors to discharge in sequence would provide an important control knob for discharge development. The immediate improvement would be that the size of the capacitor bank can be varied between shots without the need for a time consuming controlled access. The second benefit is that it would give greater control of absorber arcs as fewer capacitors could be used for injector flux conditions that require fewer capacitors. Under changing electrode conditions, such as when Lithium is deposited, having the capability to discharge three small banks separated in time by about 1ms, would allow the injector voltage to be maintained at a higher level for longer durations, as required for the transient CHI start-up process. This upgrade has now been completed and has significantly contributed to successful coupling of CHI started discharges to induction.

5. Metal divertor plates

Results from 2008 show low-z contamination of the CHI discharge to be a severe limitation for increasing the amount of CHI started current that can be coupled to induction . As shown in Figure 6.4.7, as the number of capacitors for initiating the CHI discharge are increased, the radiated power increases and there is increased line radiation from carbon and oxygen. This is a well known result from HIT-II, which shows decreased coupling to induction at increased levels of radiated power. Spheromaks operating with metal electrodes have shown electron temperatures of 500eV. The NSTX divertor plates are relatively easy to replace. For the 2009 campaign for a test of liquid Lithium divertor, part of the lower outer divertor plates would be metallic. Replacing the lower inner plates as well would significantly help CHI discharges by increasing the plasma electron temperature and allowing a high current CHI target to be generated at less

levels of radiated power. This hardware improvement in addition to the 350kW ECH system is very likely necessary to utilize the full potential of CHI in NSTX.

6. Operation at higher toroidal field

Results from HIT-II (Figure 6.4.8) clearly show that in order to maximize the closed flux current the toroidal field had to be increased. Although it is the injected poloidal flux that is responsible for increasing the closed flux current, the toroidal field plays a very significant role by reducing the magnitude of the injector current at which a given amount of poloidal flux could be injected. For reducing electrode erosion, the injector current needs to be reduced. Thus by operating at the highest possible toroidal field, the injector current could be reduced to the lowest possible value. However, as shown in Figure 6.4.8, some increases to the capacitor bank charging voltage are needed to compensate for the increased injector impedance. Thus, as part of the NSTX center stack upgrade, which would double the toroidal field, if metallic divertor plates could be used along with a small increase in the capacitor bank voltage, the total closed flux current that could be realized on NSTX could exceed 500kA. The PF1B coil which largely determines the magnitude of the injector flux is now typically operated at 5kA resulting in a closed flux current of 160kA. The maximum rating for this coil is 20kA, which means that closed flux currents in excess of 500kA should be possible in NSTX. At this current level, NBI can directly couple to the CHI produced current, thereby avoiding the intermediate step of a HHFW ramp to increase the current from 300kA to 500kA. Achieving 500kA startup currents in NSTX would make it much easier for NSTX to realize the goal of full solenoid-free start-up, ramp-up and sustainment.

Plans for 2009 - 2013

Start-up and sustainment: In this approach a transient CHI equilibrium will be produced and induction from the central solenoid will be added to this startup plasma to demonstrate compatibility of the CHI discharge with plasmas conventionally produced using the inductive method. In subsequent experiments, the CHI-started plasma will be driven inductively using a combination of outer poloidal field coils in conjunction with RF and NBI to ramp the initial startup current to a level where it can be non-inductively driven by neutral beams and by High Harmonic Fast Waves.

Edge current drive: The CHI process initially drives current in the edge, whereas other non-inductive methods drive current in the interior of the plasma. This unique capability of CHI will be used to drive steady-state current at the edge of a pre-formed inductive discharge in NSTX for the purpose of improving the edge current profile and controlling edge SOL flows for the purpose of altering the SOL density. Based on the results of these experiments, in dedicated experiments the physics of relaxation current drive may be studied as this has the potential of increasing the CHI produced current beyond what is possible using transient CHI.

Coupling to OH: Work conducted during 2008 in NSTX has conclusively demonstrated the coupling of CHI started discharges to inductive drive from the central solenoid. The remaining steps are (1) to increase the magnitude of this current to about 500kA, using higher voltage capability and higher TF of up to 1T (2) to heat the CHI started discharge with 350kW of ECH so that the electron temperature is increased above 200eV, 3) at this temperature, HHFW should be able to further increase the temperature to about 1keV, 4) At 500kA NBI should be able to ramp the current up to several hundred kA and to sustain it non-inductively.

Coupling to a pre-charged OH coil: During 2008, preliminary work with a pre-charged solenoid showed a CHI discharge could be initiated under conditions when the OH introduces fringing error fields. These discharges will be improved to enable start up under this condition.

Edge current drive for a high beta NSTX discharge: The goals are to determine the magnitude of edge current that can be added without confinement degradation and to alter the SOL flows to control the SOL plasma density. Since CHI current drive is applied to the edge region, it is possible that this current drive method can be used to modify the bootstrap current drive profile by providing current drive in regions where conventional methods cannot provide current drive. Initial experiments will use the transient CHI capacitor bank to apply voltage to the lower divertor legs of a reference inductive discharge. The purpose is to try to duplicate the experiments conducted on HIT-II, but with much improved diagnostics. If experiments with the capacitor bank are promising, then the applied current pulse would be extended using the DC power supply so that the duration of the edge current can be prolonged. Reducing the SOL density has the potential to increase the edge pedestal temperature during H-mode discharges. These experiments would be conducted after improved EMI noise suppression in the magnetic sensors and flux

loops used for plasma position control. If these, experiments are successful, relaxation current drive would be studied by using long-pulse high-current CHI discharge for initiating the plasma. Experimental data produced as part of this work is needed in conjunction with computational modeling work carried out by X. Tang of LANL and C. Sovenic of the University of Wisconsin to develop an understanding of relaxation current drive physics [18, 19]. Steady state CHI experiments thus far have succeed in attaining 390kA of CHI generated toroidal current in 330ms discharges using about 28kA of injector current. These discharges will provide data for a more complete understanding of dynamo current drive physics.

Timeline

2009

- Test heated metal outer divertor plate as cathode (reverse TF)
- Use the CHI Absorber coils to reduce the intensity of absorber arcs
- Test use of liquid Li for performance improvement

2010

- Consider 2kV capability to increase the magnitude of the CHI started currents
- Test edge current drive

2011

- Use 10ms, 350kW ECH to heat CHI plasma for coupling to HHFW
- Consider full metal divertor plates to improve CHI current startup capability
- Test relaxation current drive.

2012

- Operate at 1T to maximize CHI startup currents
- Maximize startup currents using synergism with outer PF coil startup

2013

- Use CHI startup for full integration with nearly full non-inductive operation, which includes startup with CHI, reaching Ip ~500kA followed by ramp-up with HHFW and NBI to current levels where it is non-inductively sustained.

Conclusions and Discussions – The CHI program plan on NSTX consists of two parts. For solenoid-free plasma startup, the transient CHI approach will be used. This method was demonstrated on HIT-II, and on HIT-II CHI started discharges are more robust than inductive only discharges, and they couple to and improve the performance of inductive only plasmas. Using this method, thus far 160kA of closed flux current has been produced in NSTX, which is a world record for non-inductive closed flux current generation. In addition, CHI started discharges have now successfully coupled to induction, transitioning to an H-mode and clearly demonstrating the capability of this startup method with high performance plasma operation.

Much of the needed technical development and hardware improvements needed to correctly implement this method on NSTX has been completed. A few remaining hardware upgrades remain. These are: (a) The use of metal divertor plates to reduce low-z impurity radiation during startup, (2) operation at 1T and at higher voltage to increase the magnitude of the plasma startup currents, and (3) test of synergism between CHI and outer PF startup to maximize the magnitude of startup currents.

Scaling to future devices is attractive. A number of particular importance is the injected current multiplication factor. The attained plasma current is directly proportional to this factor. It can be shown [1] that the attained plasma current in CHI discharges is given by the relation $Ip = I_{inj}[\psi_{Tor}/\psi_{Pol}]$. Here I_{inj} is the injector current, ψ_{Tor} is the toroidal flux that is inside the separatrix and ψ_{Pol} is the injector poloidal flux. For a given value of the injector flux, by increasing the toroidal flux (through increased B_T), the current multiplication factor is increased. Thus operating CHI at higher B_T is easier. The remarkable benefit of the external toroidal field can be realized by comparing CHI discharges in STs and in Spheromaks. In Spheromaks (where B_T is small) the typical current multiplication factor is about 2 to 3, which means that the injector current is nearly half the value of the plasma current. On HIT-II this ratio was increased to 6 and on NSTX it increased to a remarkable 60. HIT-II has consistently operated at an injector current of 30kA and produced CHI discharges that coupled to and improved the performance of inductive discharges. For a machine such as CTF, a similar level of current density as on HIT-II would allow the injector to be operated at 250kA of injector current. The toroidal flux in CTF is about five times that in the present NSTX, which means that the current multiplication factor would be at least that achieved on NSTX. At a conservative value of the injector current of 50kA and current multiplication factor of 50, CTF should be able to realize plasma startup currents in excess of 2MA.

6.4.2 Plasma Start-up Using Outer Poloidal Field Coils

Because of the criticality of the OH-solenoid-free start-up issue for ST research, the NSTX PAC has urged the NSTX team to pursue alternate methods of OH-solenoid-free start-up. This method uses the external poloidal field coils to induce a toroidal electric field. It has been successfully used on the START and MAST devices [20]. In both these devices the poloidal field coils are located inside the vacuum vessel. NSTX will conduct these experiments in a configuration in which the PF coils are located outside the vacuum vessel. Initial results are promising and the potential for the generation of up to 500kA of toroidal current exists in NSTX [21-23]. This method could also work with an initial CHI or Plasma-Gun produced plasma to further boost the level of solenoid-free current generation.

Introduction **-** In addition to CHI, NSTX will investigate a concept for solenoid-free inductive plasma startup utilizing only the outer poloidal-field coils. We describe an experimental setup for generating up to 500 hundred kilo amperes of plasma current in NSTX by this method. Such plasma would provide a suitable starting point for the non-inductive current ramp-up experiments. If successful, this concept is applicable as a possible start-up method for the NHTX (Next Step ST) device [24], and will provide a crucial element for future ST-based nuclear facilities, such as the Component Test Facility (CTF) [25].

The MAST experiment routinely uses poloidal field coils at a larger major radius than the plasma but still inside the vacuum chamber to initiate the plasma; however, to be able to extrapolate the technique to future experiments, and fusion energy systems, it would be advantageous to use only the poloidal field coils located outside the vacuum vessel wall for startup.

Basic Concept of the Plasma-Start-Up with Outer Poloidal Coil System **-** Using only the outer PF coils of NSTX, we are able to satisfy the conditions for plasma start-up which have been established by many previous experiments using a conventional central solenoid. There are three important conditions which need to be satisfied for inductive startup:

1. A region of low poloidal magnetic field must be created over a sufficiently large region of the vacuum vessel poloidal cross-section to allow the ionization avalanche to develop in the applied toroidal electric field. The condition for highly reliable breakdown can be expressed as $E_T \cdot B_T / B_P >$ ~1 kV/m, where E_T is the induced toroidal electric field, B_T is the toroidal magnetic field and B_P is the

average poloidal (*i.e.* transverse) magnetic field. However, the application of suitable rf waves to break down the gas can relax this condition. For example, on DIII-D, operating at B_T = 2 T, with high-power ECH pre-ionization (~ 800 kW), start-up was achieved at E_T = 0.3 V/m with B_P > 5 mT over most of the vessel cross-section [19]. This represents a value of $E_T \cdot B_T / B_P \approx 0.12$ kV/m. The benefit of pre-ionization with even a very small ECH power (~ 20 kW) has been shown on NSTX (and also on other ST devices including CDX-U, START, MAST, and PEGASUS) [20]. The proposed configuration for NSTX startup achieves $E_T \cdot B_T / B_P \sim 0.12$ kV/m, comparable to the value achieved on DIII-D.

2. The field null, which is produced transiently by the combined effects of currents in the PF coils and the induced currents in the machine structure, must be maintained for a sufficient duration ~ 3 milliseconds to develop the avalanche. DIII-D experiment found that the time required increased as the loop voltage was reduced. However, high power ECH pre-ionization (~ 800 kW) was able to shorten this process on DIII-D to ~ 2 msec even at low loop voltage. The field null is maintained in the proposed NSTX startup configuration for 3 msec.

3. After breakdown, the poloidal field coils must provide both fields to maintain plasma equilibrium and sufficient flux change for the current to ramp up to the desired level. The change in the vertical field required for equilibrium produces additional flux during the current ramp-up. These requirements are met in the proposed configuration.

Outer Poloidal Field Start-Up Configuration on NSTX – We propose to utilize the existing poloidal coil sets and available power supplies on NSTX for solenoid-free start-up. In Figure 6.4.11 (a) the poloidal coils installed on NSTX are shown. The required current levels in Figure 6.4.11 (a) are consistent with the current rating of the coils and power supplies for the short durations needed for this experiment. The mid-plane vertical field generated by the combination of PFs 2, 3, and 5 is compared with that generated by PF 4 in Figure 6.4.11 (b). The combined field is shown in Figure 6.4.11 (c); the field null is created around R = 1.4 m. In Figure 6.4.12 (a), the resulting two dimensional poloidal field contours are shown. As can be seen in Figure 6.4.12 (a), a high quality field null is created. From Figure 6.4.12 (b), one can see that about 0.16 Wb (at R =

1.0 m) is available for the current ramp up for this particular set of coil currents. In NSTX, under an optimized condition, about 0.3 Wb from the solenoid can produce a 1 MA discharge. Thus, the 0.16 Wb flux swing available from this scenario at R ≈ 1.0 m could, in principle, produce plasma currents of order 0.5 MA.

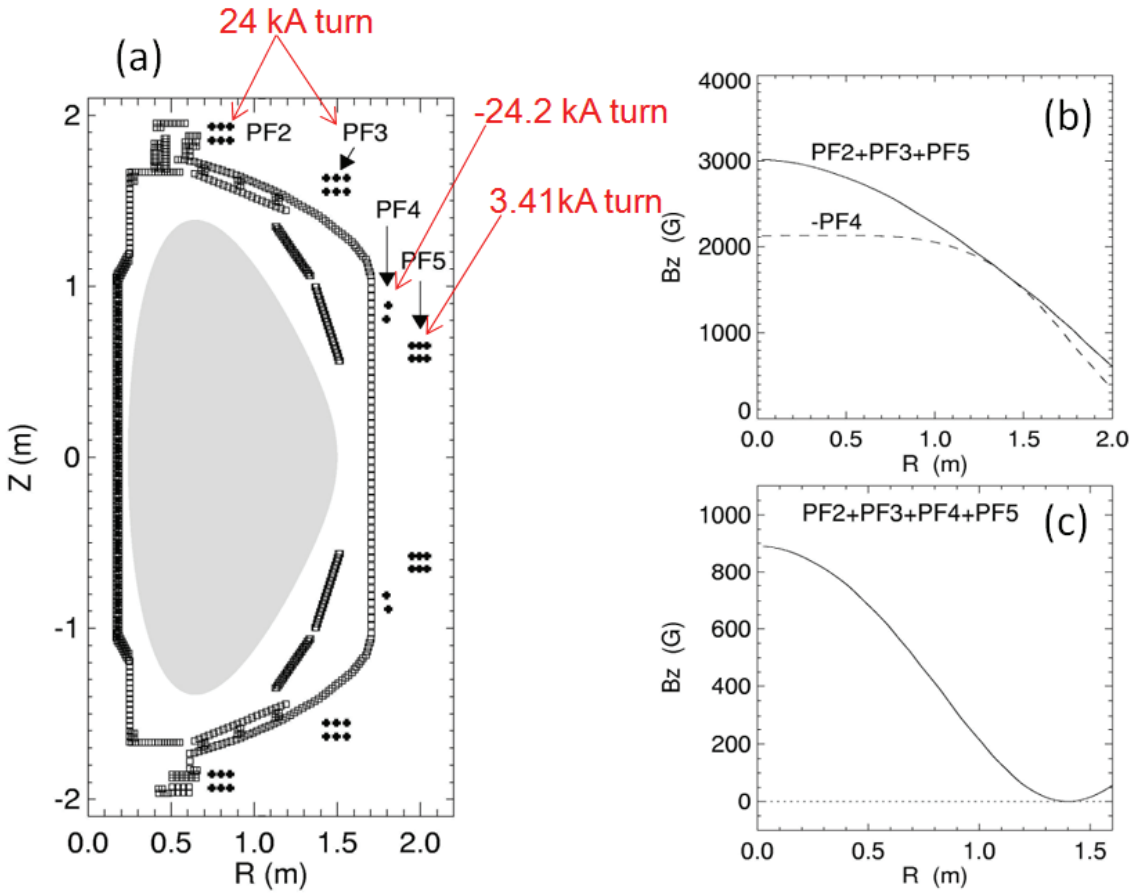

Figure 6.4.11: NSTX Configuration. (a) A schematic of the NSTX poloidal field coil set up. The required coil currents are indicated. (b) The mid-plane vertical field for the combination of PFs #2,#3 and#5 and PF #4. (c) The mid-plane vertical field generated by PFs 2, 3, 4, and 5

Pre-Ionization – On NSTX, start-up has been routinely achieved for a relatively low loop voltage of ~ 2 V with ECH pre-ionization. For the outer-PF-only start-up scenario, we expect to be able to generate a loop voltage up to 6 V transiently, corresponding to a toroidal electric field of 0.7 V/m at the radius of the field null, R = 1.4 m. The toroidal field there is up to 0.35 T. Within the broad region where the poloidal field is < 20 G, the value of $E_T \cdot B_T / B_P$ is above 0.12 kV/m. Since DIII-D was able to initiate the plasma for $E_T \cdot B_T / B_P$ as low as this value with strong ECH pre-ionization, start-up should be also feasible in NSTX if adequate pre-ionization is provided. For NSTX, with a combination of ECH (~ 20 kW) and HHFW (~ 1 MW), a favorable pre-ionization condition may be created. On CDX-U, this combined ECH-HHFW technique was indeed shown to be effective in creating relatively robust preionized plasmas [27].

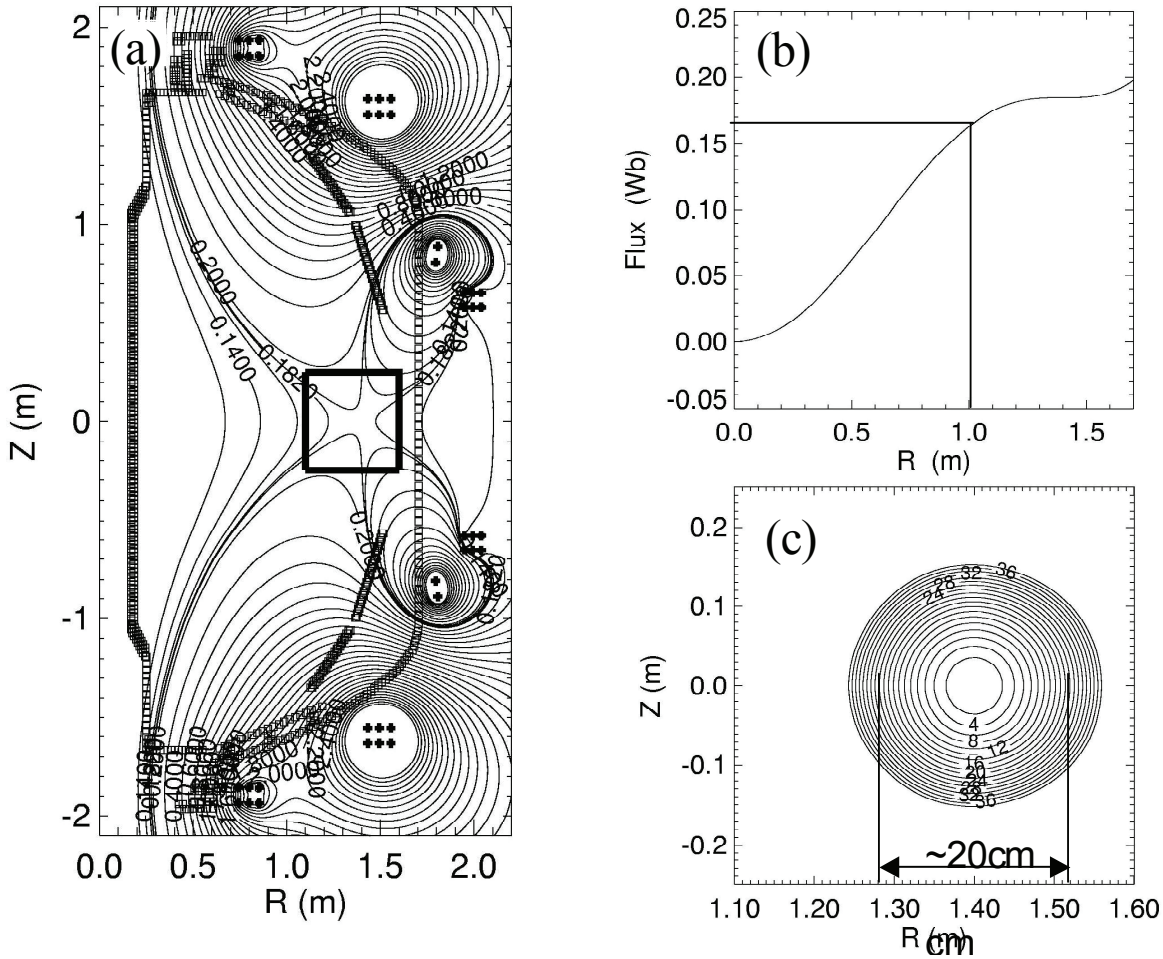

Figure 6.4.12: The NSTX null-field configurations. (a) Flux contours. (b) Flux radial profile. (c) Mod-B surfaces of the field null region

This preionization can be further developed and its effectiveness tested in the near term on NSTX using the existing ECH and multi-MW HHFW system. An initial test using these pre-ionization methods allowed the production of up to 20 kA of plasma current, as shown in Figure 6.4.13. The primary findings are that the 20 kW of ECH is too small and that HHFW is not a good pre-ionizing system. The experiment will be attempted again in 2009 using CHI for preionization and in 2011 after the installation of the 350 kW ECH system. In addition to this a washer plasma gun source will be installed for 2010. This may inject adequate amounts of ionized plasma into the field null region, which should facilitate easier breakdown of the remaining neutral gas. A Compact Toroid (CT) injector is also being considered for Advanced Fuelling experiments. This has the potential to inject all of the required plasma directly into the field null region, and is a possibility for experiments beyond 2012.

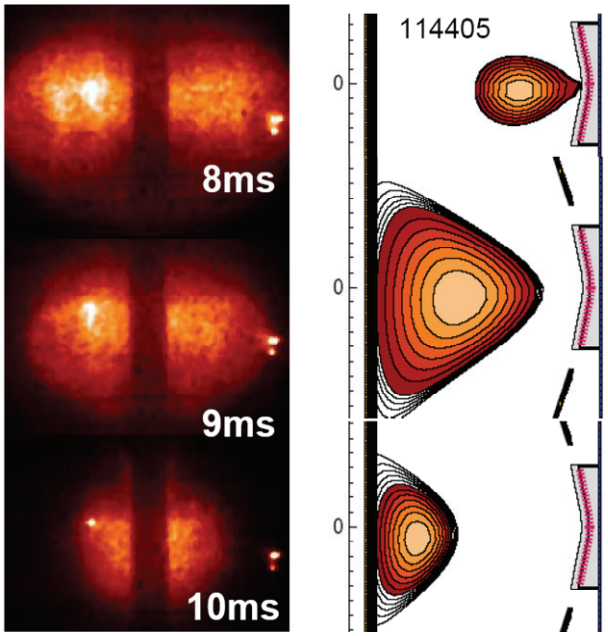

Figure 6.4.13: Shown on the left are fast camera fish eye visible images of a discharge produced using outer PF start-up. A small bore plasma is formed in the outer region as show by LRDFIT reconstruction at 8ms (top right), that subsequently moves to the inner wall and decays over several 10s of ms. Up to 20kA of plasma current was generated.

Maintenance of Field Null – During the initiation, it is important to maintain the field null for about 3 ms to create the avalanche. Since the poloidal field is changing rapidly during this period and inducing significant vacuum vessel eddy currents, a dynamic modeling code to include the vacuum vessel eddy currents has been implemented. This analysis shows that it is indeed possible to maintain the field null for about 3 ms, which should be long enough to initiate the avalanche process with the aid of sufficient pre-ionization as described above. The plasma stability with the presence of the eddy currents is an issue that needs to be further investigated. The presence of the nearby passive plates in NSTX should aid the vertical stability.

Hardware and Modeling Requirements

for Outer PF startup

The current ramp up will require PF 5 to provide much of the equilibrium vertical field. However, for the initial test of the concept, the crucial initial breakdown and avalanche process was tested by reversing the PF 5 connection to its existing power supply. The bi-polar capability will be implemented after further tests. Once the plasma initiation is successful, feedback control must be introduced to maintain the plasma equilibrium and shape during the current ramp-up. The TSC code [28] will be utilized for the development of suitable current ramp-up scenarios to guide the development of control algorithms.

Plans for 2009 – 2013

2008: Preparatory work scopes:

- Continue the basic start-up calculations including the wall eddy currents
- Assess basic power supply reconfigurations
- Analyze electro-magnetic forces and needs (if any) for further bracing of PF coils.

2009: Initial Plasma Initiation Experiments with CHI

- Develop effective pre-ionization capability using the CHI system with some assist from the central solenoid.
- Conduct initial breakdown and current initiation experiment up to ~ 100 kA with using the existing uni-polar supply for PF 5.
- After confirming successful breakdown, implement needed hardware changes including the bi-polar capability of PF 5.
- Develop optimized current ramp-up scenarios using TSC.
- Develop required magnetic sensors and control algorithms based on the TSC simulation.

2010: Initial Plasma Initiation Experiments with plasma guns

- Develop effective pre-ionization capability using the washer gun plasma sources with some assist from the central solenoid.

2011: Start-up Demonstration Experiments with ECH

- Establish a few hundred (Ip ~ 300 - 500 kA) plasma discharges without use of the OH solenoid and higher power HHFW after using the newly installed ECH system for pre-ionization.
- Apply HHFW and/or NBI to achieve high beta poloidal discharges without the OH solenoid.
- Develop comprehensive understanding and predictive capabilities of the outer poloidal field coil plasma start-up concept for future devices including NHTX.

2012-13: Assist the non-inductive research as a tool for ohmic-solenoid-free start-up.

- Using a combination of CHI start-up and outer PF start up or Plasma Gun start-up and outer PF start-up, ramp-up to a high beta target.

Conclusions and Discussions – A plasma start-up concept using only the outer PF coils has been introduced. This method appears capable of generating in NSTX a solenoid-free start-up current of a few hundred kilo amperes, comparable to that produced by CHI. Once a significant level of plasma current is established, it should be possible to use other means of non-inductive current drive such as the bootstrap over-drive, and/or NBI / RF current drive to further ramp up and maintain the current. The outer PF coil start-up concept can be implemented relatively quickly with minimal facility modifications and, if successful, can play an important role in the non-inductive research phase of NSTX as described in this Five-Year plan. The concept scales favorably toward larger and higher field devices, such as NHTX, since the higher field tends to ease the breakdown requirements and the amount of available flux scales with the square of the major radius and linearly with the field. If successful, it will give us a method for the ohmic-solenoid-free start-up of future ST devices to a significant level of plasma current.

6.4.3 Plasma Gun Startup

In this method an electron beam is driven along magnetic filaments using a washer gun plasma source [3]. The method was first tried on the CDX-U machine [29] with some success. More recently the method has been further developed on the PEGASUS ST [30]. On Pegasus 30 kA of gun generated toroidal current was produced and ramped up to 80 kA after coupling to induction. The method has the advantage that it could be easily implemented in a reactor as the gun sources could be withdrawn after current generation. NSTX will test the viability of this concept in a large ST [31].

Introduction - In this method, an electron beam is created by biasing a washer gun plasma source negative with respect to the external vessel or a floating probe inserted into the vacuum chamber. An appropriate vacuum magnetic field pattern is setup so that the combination of poloidal and toroidal fields creates a spiraling field line configuration. The electrons released by the gun then follow these field lines. This method now adopted by PEGASUS is an improvement over the early experiments on CDX-U [30], in that CDX-U used a heated Lanthanum Hexaboroide cathode, which from a cleanliness point of view is probably less cleaner than the plasma gun sources. In the Plasma gun sources, by choosing the appropriate bias voltages, the ions released by the gun can be made to preferentially fall back into the gun cavity, thereby reducing impurity influx into the vessel. These plasma gun sources typically operate for about 10 ms, which is about the time needed to couple it to induction from the outer PF coils.

Results from Pegasus

At present two different experiments have been performed on Pegasus. In the initial experiment, the gun source was located near the lower divertor region. It was then biased with respect to a floating component positioned below the upper divertor, so that an electron beam was driven up as shown in Figure 6.4.14. At sufficient low values of the toroidal field the spiraling electron beam channel relaxed and merged to a diffuse current channel that filled the entire vessel as shown in right portion of Figure 6.4.14. In these experiments up to 50 kA of toroidal current was generated using 4 kA of gun current. For representative cases, the toroidal field was about 0.01 T and the vertical field was 0.005 T.

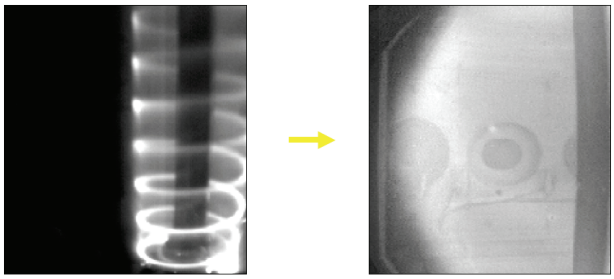

Figure 6.4.14: Visible images of the current channel prior to and after relaxation in Pegasus Washer Gun experiments.

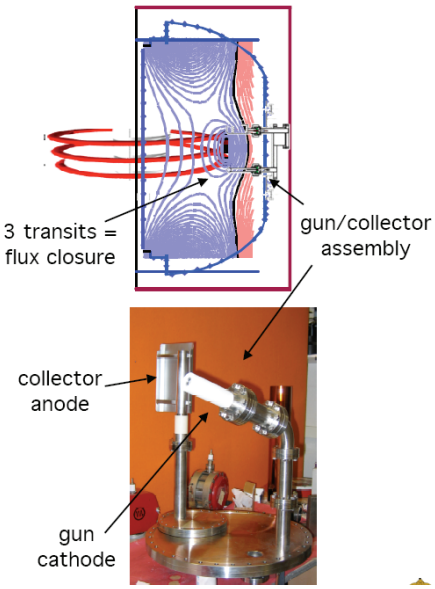

Figure 6.4.15: Layout of the mid-plane gun injection system in Pegasus

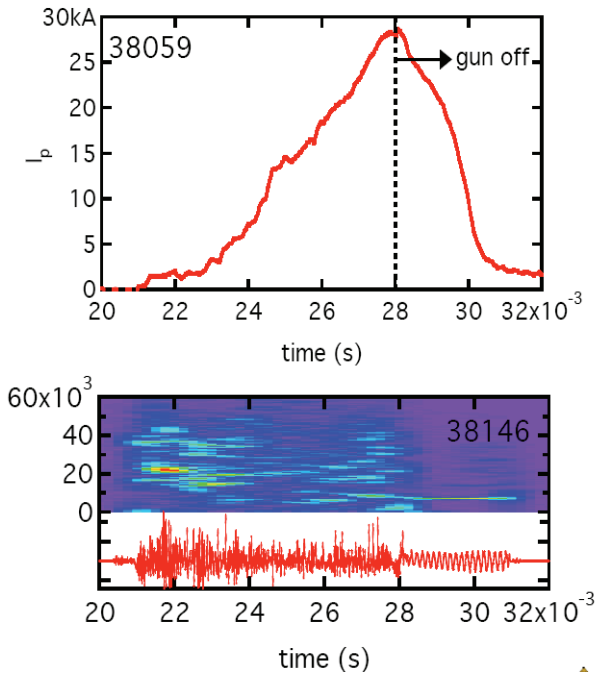

Figure 6.4.16: Plasma current and MHD activity of a discharge during mid-plane gun injection experiments in Pegasus.

In more recent experiments of perhaps more relevance to NSTX, the gun and a collector assembly was mounted in the outer midplane as shown in Figure 6.4.15. The driven electron channel now occupied the outer midplane of the vessel. In these experiments at relatively higher values of the toroidal field, up to 25 kA of toroidal current was generated using 1.5 kA of gun current as shown in Figure 6.4.16. After the guns were turned off, the current persisted for 2 ms and was accompanied by coherent MHD activity indicative of the generation of closed flux. When this discharge was coupled to induction from the central solenoid, the current ramped up beyond what was possible using induction alone showing coupling to induction, as seen in Figure 6.4.17.

Implementation of the method in NSTX

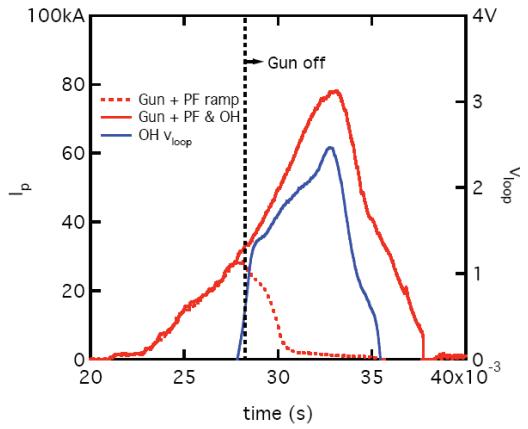

Figure 6.4.17: Shown are in blue an OH only discharge and in red, the same preprogrammed loop voltage applied to a mid-plane gun generated plasma.

The method will be implemented on NSTX in a manner similar to the Pegasus mid-plane experiments. A design of the conceptual design is now underway by the Pegasus group.

Schedule (2009 to 2013)

2008-09: Conduct supporting experiments on Pegasus to understand scaling to larger current levels. Design the system for NSTX, including identifying hardware components and installation details.

2010: Installation on NSTX and commissioning tests. Support outer PF start-up experiments, by injecting ionized plasma into the region of field null. Test to see if the startup loop voltage on NSTX can be reduced as a result of gun injected pre-ionized plasma.

2011: Test of plasma startup using the guns installed in the gap region between the primary and secondary passive plates.

2012-2013: Based on 2011 results, upgrade the system to produce higher current levels.

Conclusion and Remarks:

The method is simple in concept and could be easily adapted to larger machines as the gun sources could be withdrawn after plasma startup. Initial results from Pegasus are encouraging. NSTX will test the concept on a larger scale. The method is compatible with outer PF startup and will assist the outer PF startup experiments by providing a pre-ionized source of plasma.

6.4.4 Plasma Current Ramp-up

Non-solenoidal initiation and current ramp-up is a critical goal of the ST program since its attractiveness is directly tied to eliminating or minimizing the inductive central solenoid on the inboard side of the device and allowing access to compact geometry. Since none of the proposed solenoid-free current start-up methods are expected to generate the full magnitude of the nominal value of the steady-state plasma current of a device like ST-CTF, successful demonstration of methods for non-inductive current ramp-up are essential to meet the goals of the ST program. As previously described, a discharge to achieve this goal can be divided into three phases; the breakdown and startup with coaxial helicity injection or the outer poloidal field PF coils or Plasma Gun startup as described in sections 6.4.1 to 6.4.3. The second phase is the current ramp-up phase. During this phase the current magnitude is non-inductively increased to the levels needed for steady-state operation. For NSTX plasmas, the early plasma current ramp-up and heating would be achieved with HHFW, and the later plasma current ramp-up and heating would be achieved using both HHFW and NBI [32]. In next-step devices it might in principle be possible to perform the ramp-up with NBI alone, but sufficient plasma current and density are required to avoid fast-ion loss and shine-through, respectively, so wave heating may remain useful or even necessary in next-steps. It is useful to note that the requirements on the non-inductive current ramp-up systems could be reduced if the initial current produced during the start-up phase is increased. During the final sustainment phase, a combination of bootstrap current drive, neutral beam and RF current drive are expected to maintain the current at steady state values. The time scales required for non-inductive current ramp-up are long compared to those required with inductive current ramp-up, since the inductive ramp rate is limited by the current redistribution time at the plasma edge whereas the non-inductive current ramp rate is limited by the current redistribution time at the plasma center [33].

To understand the requirements of current ramp-up, the TSC code has been used to establish the requirements of HHFW and NBI power and energy and the required target plasma conditions (density, temperature, current and magnetic field levels) and the simulations discussed below are described more extensively in Reference 32. The simulations assume that the plasma starts the non-inductive ramp-up at I_P=100 kA, provided by the initiation phase, which is treated in the code as inductive current. HHFW is the heating and current drive source in this low I_p and low T_e phase, and NBI is added in the higher I_P phase when the I_P rate of increase is slowing down. The toroidal field is 0.45 T allowing a maximum of 1.8s of pulse length. In the low I_P phase the HHFW power is ramped slowly to avoid current hole formation, whereas the density is ramped to keep the temperature sufficiently low to access short core

current redistribution time scales. In order to keep the temperature from increasing too fast in this phase the plasma is limited on the inboard wall to avoid transition to H mode. The peak electron temperature reaches 1.3keV, whereas the density ramps up to $0.3x10^{20}m^{-3}$ over 0.3s. Around 0.3–0.4s the plasma is diverted, allowing an improvement in global confinement. Then beginning at 0.5s 6MW of NBI power is injected in steps, accounting for the poor beam fast ion confinement at these lower plasma currents. The NB power absorbed and subsequent driven current is based on the beam confinement observed in the I_P ramp-up in discharge 109070 from TRANSP. The heating and driven current from the beam continue to improve as the plasma current increases, but the slow current rise keeps the absorbed power low in these simulations, only reaching 2–3MW for 6MW of injected power. The poloidal beta reaches 2.8, the toroidal beta reaches about 5.0, li(1) drops to 0.47, and the central safety factor remains above 4.0 during the discharge simulation. The bootstrap current reaches 300kA, and the HHFW driven current maximizes at 150kA in the early phase and decreases when the density rises and NB fast ions are present to absorb HHFW power calculated by CURRAY. The HHFW phase is $7m^{-1}$ co-CD (same direction as the plasma current) and up to 6 MW are injected. By 1.8s the total plasma current has reached just over 420kA. As the beam ions are not well confined, at these low plasma currents a significant HHFW current persists, in spite of parasitic absorption of HHFW power on fast NB ions. These results are shown in Fig. 6.4.18 giving the contributions to the plasma current, density and electron and ion peak temperatures as a function of time. The present NSTX does not have sufficient pulse length to reach a plasma current of at least 800kA to connect to a high performance plasma configuration, but can demonstrate the critical features of the non-inductive ramp-up.

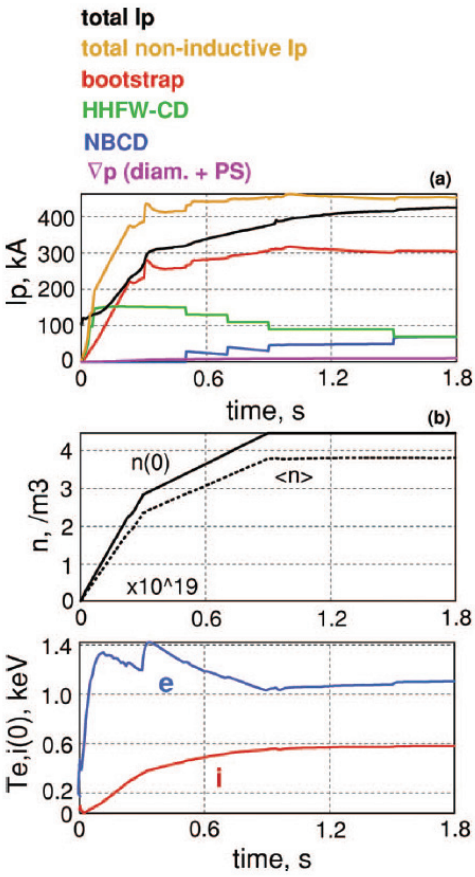

Figure 6.4.18: (a) Time histories of the plasma current (black), the total non-inductive current (yellow), and the contributions to the plasma current from bootstrap (red), HHFW CD (green), and NBCD (blue). (b) The peak electron and ion temperatures, and electron density for the non-solenoidal Ip ramp-up simulation for NSTX at B_T=0.45T.

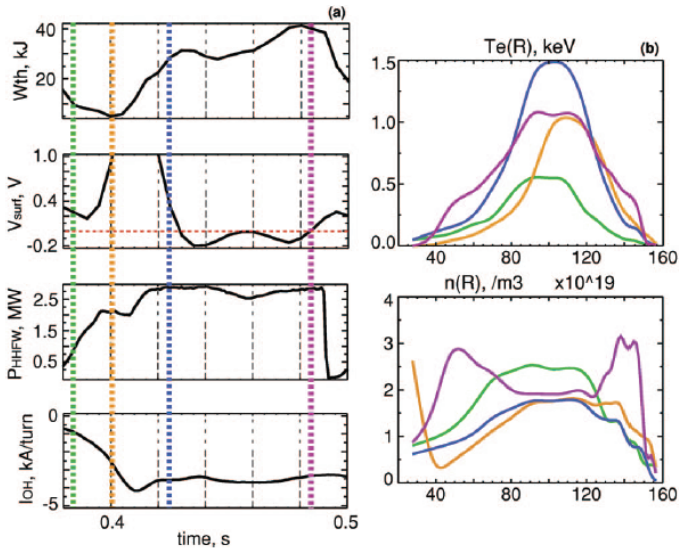

Figure 6.4.19: (a) Experimental time traces of the stored energy, surface voltage, injected HHFW power, and solenoid current during a segment of discharge 117605. (b) The electron temperature and density profiles as function of major radius at the time slices indicated on the time traces, 0.385 (green), 0.400 (yellow), 0.425 (blue), and 0.485 s (pink).

Experiments have begun to examine the HHFW heating and current drive at low I_P. Shown in Fig. 6.4.19 is a segment of a discharge where the plasma current was ramped up and maintained at 250 kA with the solenoid. Up to 2.8 MW of HHFW power was injected with $k_{||}$=14 m^{-1} heating phase in an effort to drive the surface voltage to 0. The injection of power drives the stored energy up significantly and creates an H-mode confinement regime. The surface voltage is reduced to 0 or even slightly below, and the solenoid current becomes slightly inverted or flat indicating it is no longer providing volt seconds to the plasma. Also shown in Fig. 6.4.19 are the electron temperature and density profiles at four time slices indicated on the time history plots. The starting profile shows the peak electron temperature of about 500eV, which rises to 1.0keV over the next 0.015 s from HHFW heating. This continues with the peak temperature reaching 1.5keV and an H-mode temperature pedestal beginning to form 0.040s later. Finally after 0.10s the electron temperature profile has broadened significantly generating high pedestal temperatures, and a lower peak temperature. This particular type of profile is ideal since it will generate a large bootstrap current, but keep the central temperature low enough to allow a reasonable I_P ramp rate. Unfortunately the HHFW power was unable to be sustained due to loading mismatches due to H-mode, but future upgrades to the HHFW system are planned for 2009-10 to increase the HHFW power and make the HHFW system more resilient to H-mode and ELMs.

Importantly, with the proposed major upgrades of NSTX (new center-stack and 2nd NBI), TSC simulations indicate that non-inductive plasma current ramp-up to higher plasma current approaching 1MA is possible. Shown in Figure 6.4.20 are results from preliminary (un-optimized) TSC simulations in which the toroidal field was increased to 1T in combination with increased NBI power and duration made possible by the addition of the second NBI source. As shown in the Figure, starting from 300ms with a plasma current level of 350kA, a constant HHFW power at 6MW is utilized to heat the target plasma and ramp the initial current non-inductively to a value where the NBI should begin to be absorbed efficiently. Starting at 500ms, the neutral beam power is increased in steps as for the simulations shown in Figure 6.4.18. Near the end of the simulations shown in Figure 6.4.20 the internal inductance begins to increase and the central q and electron density are not yet stationary. Thus, although these simulations show the significant benefit of higher TF and NBI power for non-inductive ramp-up, additional work is needed to optimize the long-time-scale discharge evolution. Additional TRANSP simulations are also needed to ensure that NBI is adequately absorbed in the lowest current phase of the ramp-up. Finally, it is important to note that the current ramp-up to 800-850kA takes up to 3s in these simulations. Thus, the ability to sustain 1T toroidal field and 7-8MW NBI heating for at least 3s is essential to demonstrate ramp-up to currents in the ~1MA range, and these capabilities are only possible with the proposed major upgrades to NSTX.

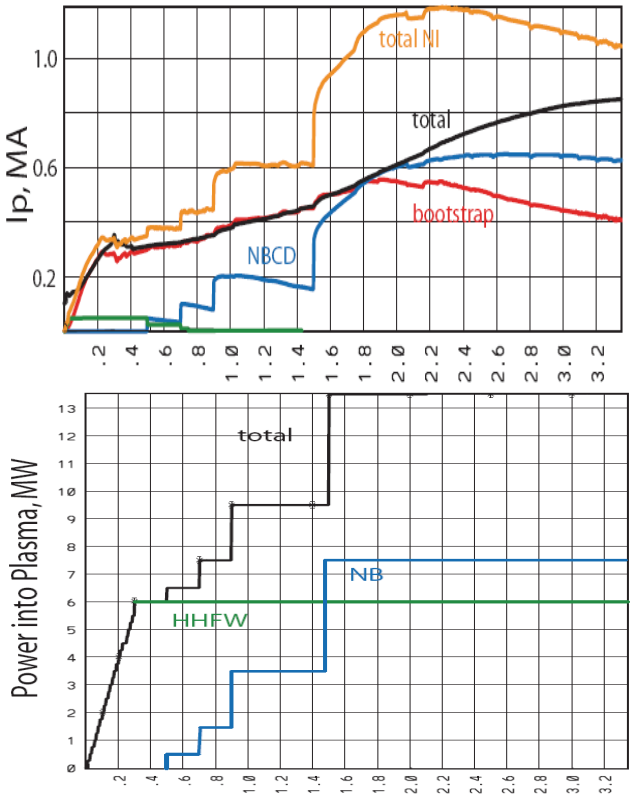

Figure 6.4.20: Current ramp up results from the TSC code at a toroidal filed of 1T and with 7.7MW NBI and 6MW HHFW (plasma absorbed power)

Plasma Current Ramp-up Research Plan for 2009 to 2013

2008

Conduct supporting experiments on heating deuterium discharges in NSTX to access H-mode and to understand HHFW coupling in deuterium plasmas.

2009-11

In conjunction with TSC simulations, experimentally test and understand the minimum levels of plasma current required for current ramp-up using the higher power capability of HHFW. A FY10 HHFW milestone is to use higher power HHFW and ELM resilience to attempt Ip ramp-up from 200-250kA to 400-500kA using HHFW heating and current drive and bootstrap current drive.

2012

1T expected to reduce the normalized beta required to achieve high bootstrap fraction for overdrive, also expected to increase target Te for increased HHFW absorption and higher CD efficiency. NBI also should become more effective at higher field and current.

2013

Measure the extent of current ramp-up that is possible using a solenoid-free startup target and establish initial current startup requirements for full non-inductive ramp-up. (Incremental funding): Utilize 2nd NBI to increase absorbed NBI power and sustain high NBI power (7-8MW) to test solenoid-free ramp-up to ~800kA within 3-5s.

2009 – 2013 Timeline for Plasma Current Start-up and Ramp-up Research

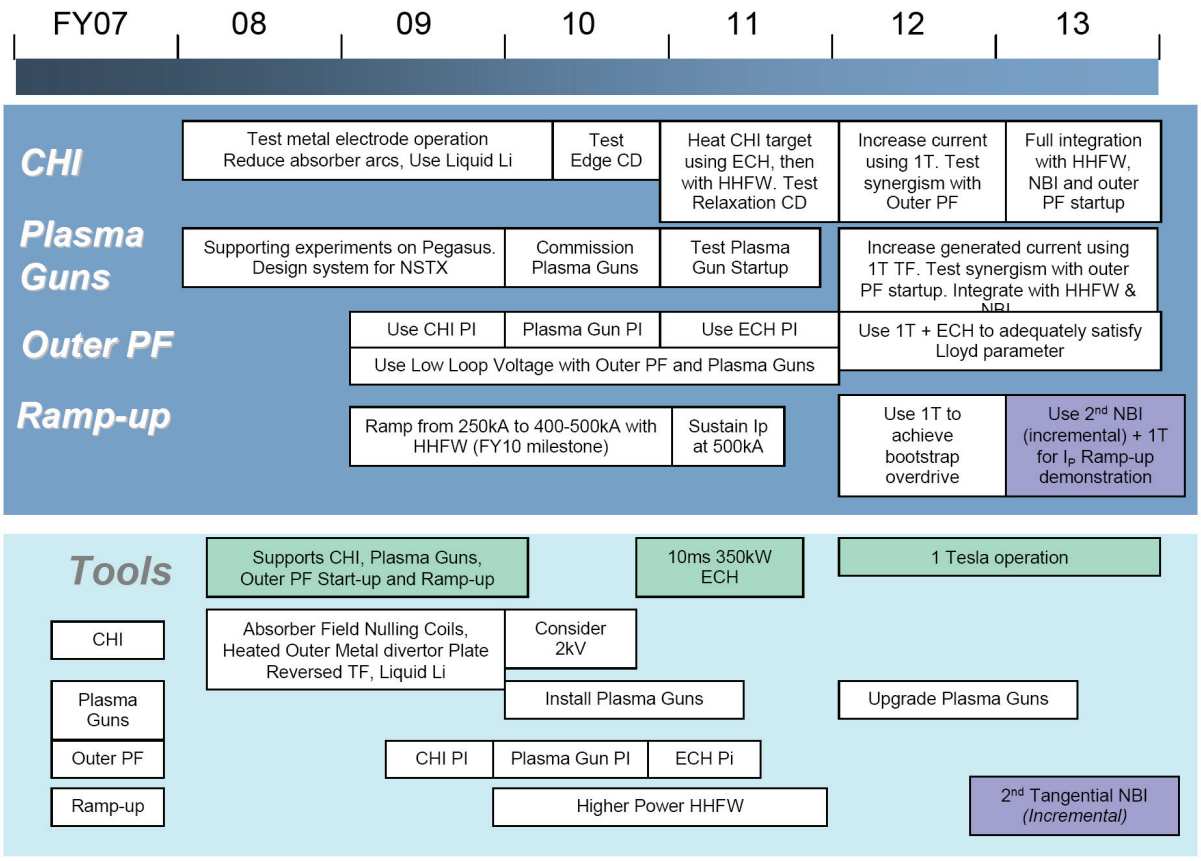

References

[1] T.R. Jarboe, "Formation and steady state sustainment of a tokamak by Coaxial Helicity Injection," Fusion Tech. **15**, 7, (1989).

[2] M. Ono and W. Choe, "Out-Board "Ohmic Induction" Coil for Low-Aspect-Ratio Toroidal Plasma Start-up", Princeton University Patent Disclosure 03-2003-1.

[3] G.D. Garstka, *et al.,* "Attainment of High Normalized Current by Current Profile Manipulation in the Pegasus Toroidal Experiment," Journal of Fusion Energy, 27:20-27, DOI 10.1007/s10894-007-9094-1 (2008)

[4] C.W. Barnes, T.R. Jarboe, *et al.,* "Spheromak Formation and Operation with Background Filling gas and a Solid Flux Conserver in CTIX," Nuclear Fusion **23**(3), 267 (2984).

[5] M.J. Schaffer, et al., "Increased divertor exhaust by electrical bias in DIII-D," Nuclear Fusion, **36**, 496 (1996).

[6] Nelson, B.A., *et al.*, "Formation and sustainment of a low-aspect ratio tokamak by coaxial helicity injection," Phys. Plasmas **2** (1995) 2337.

[7] Nagata, M., *et al.*, "Helicity injection current drive of spherical tokamaks and spheromak plasmas in HIST," 17th IAEA Fusion Energy Conference, Yokohama, IAEA-CN 69/EXP4/10 (1998).

[8] Browning, P.K., *et al.*, "Injection and sustainment of plasma in a preexisting toroidal field using coaxial helicity injection," Phys. Rev. Lett. **68** (1992) 1722.

[9] Jarboe, T.R., Raman, R, Nelson, B.A., *et al.*, "Current drive experiments on the HIT-II spherical torus," 17th IAEA Fusion Energy Conference, Yokohama, IAEA-CN 69/PDP/02 (1998).

[10] R. Raman, T.R. Jarboe, B.A. Nelson, et al., "Demonstration of plasma startup by coaxial helicity injection," Phys Rev. Lett. **90**, 075005-1 (2003).

[11] R. Raman, B.A. Nelson, M.G. Bell, T.R. Jarboe, D. Mueller, T. Bigelow, B. LeBlanc, R. Maqueda, J. Menard, M. Ono, R. Wilson, Efficient generation of closed magnetic flux surfaces in a large spherical tokamak using coaxial helicity injection, Phys Rev. Lett., **97**, 175002 (2006)

[12] R. Raman, D. Mueller, et. al., "Non-inductive solenoid-less plasma current startup in NSTX using Transient CHI," Nuclear Fusion, **47** (8), 792 (2007).

[13] R. Raman, T.R. Jarboe, B.A. Nelson, W.T. Hamp, V.A. Izzo, R.G. O'Neill, A.J. Redd, P.E. Sieck and R.J. Smith, "Experimental demonstration of plasma startup by coaxial helicity injection," Phys Plasmas **11**, 2565 (2004).

[14] R. Raman, T.R. Jarboe, D. Mueller, D., *et al.*, "Non-inductive current generation in NSTX using coaxial helicity injection," Nucl. Fusion **41**, (2001) 1081.

[15] T.R. Jarboe, R. Raman, B.A. Nelson, *et al.*, "Progress with helicity injection current drive," *19th IAEA Fusion Energy Conference*, Lyon, IAEA-IC/P 10 (2002).

[16] R. Raman, T.R. Jarboe, D. Mueller, et al., "Initial results from CHI experiments in NSTX," Plasma Phys. Contrl. Fusion **43**, 305 (2001).

[17] D. Mueller, R. Raman, T.R. Jarboe, et. al., "Coaxial Helicity Injection plasma plasma start-up coupled to inductively driven sustainment on NSTX," Proc. 35th EPS Conference. Crete, Greece, 9-13 June (2008).

[18] X.Z. Tang and A.H. Boozer, "Flux amplification in helicity injected spherical tori," Phys. Plasmas 12, 042113 (2005).

[19] X.Z. Tang and A.H. Boozer, "Scale-up of spherical tokamak solenoid-free startup by coaxial helicity injection," Phys. Plasmas 14, 100704 (2007).

[20] A. Sykes, "The spherical tokamak program at Culham," Nuclear Fusion, **38**, No. 9Y, 1271 (1999).

[21] Y. Takase, et. al., "Solenoidless startup in NSTX." NSTX Research Forum, Nov 11 (2003), Princeton, NJ

[22] J.E. Menard, "HHFW-assisted PF-only startup in NSTX," NSTX Research Forum, Nov 10-11 (2003), Princeton, NJ

[23] W. Choe, J. Kim, M. Ono, "Test of outer PF coil-only inductive plasma startup technique on NSTX," NSTX Research Forum, Nov. 10-11 (2003), Princeton, NJ

[24] J. Menard, et. al., NHTX information: http://nstx.pppl.gov/DragNDrop/NHTX_Information/

[25] Y-K.M. Peng, et al., "A component test facility based on the spherical tokamak," Plasma Phys. Control. Fusion, **47** (2005) B263-B283

[26] B. Lloyd, et al., "Low voltage Ohmic and Electron Cyclotron Heating assisted startup in DIII-D," Nuclear Fusion 31, 2031 (1991)

[27] J.E. Menard, "High harmonic fast wave coupling and heating experiments in the CDX-U spherical tokamak," Ph.D. Thesis, Princeton University, June (1998).

[28] S.C. Jardin, N. Pomphrey, N. GeLucia, "Dynamic modeling of transport and position control of tokamaks," Journal of Computational Physics **66**, 481 (1986).

[29] M. Ono, et al., "Steady-state tokamak discharge via DC helicity injection," Phys. Rev. Lett., **44**, 393 (1980).

[30] A.J. Redd, et al., "Non inductive plasma startup and current profile modification in Pegasus spherical torus discharges," ICC Workshop, June 26 (2008), Reno, Nevada

[31] A. Sontag, "DC helicity injection in Pegasus," NSTX Research Forum, Nov 27 (2007), Princeton, NJ

[32] C.E. Kessel, et al., "Long pulse high performance plasma scenario development for the National Spherical Torus Experiment," Phys. Plasmas **13**, 056108 (2006)

[33] S.C. Jardin, "Timescales for non-inductive current buildup in low aspect ratio toroidal geometry," Nucl. Fusion **40**, 1101 (2000)